Journal of Hydrology: Regional Studies 18 (2018) 119–142

Contents lists available at ScienceDirect

Journal of Hydrology: Regional Studies

journal homepage: www.elsevier.com/locate/ejrh

Potential and limits of stable isotopes ($\delta^{18}O$ and δD) to detect parasitic water in sewers of oceanic climate cities

K. De Bondt[a,*], F. Seveno[b], G. Petrucci[a], F. Rodriguez[b], C. Joannis[b], Ph. Claeys[a]

[a] Analytical- Environmental- and Geo-Chemistry (AMGC), Vrije Universiteit Brussel (VUB), Belgium
[b] Laboratoire Eau et Environnement, GERS, Institut Français des Sciences et Technologies des Transports, de l'Aménagement et des Réseaux (IFSTTAR), F-Bouguenais, France

ARTICLE INFO

Keywords:
$\delta^{18}O$
δD
Stable isotopes
Parasitic water
Groundwater
Waste-water inflows
Sewers

ABSTRACT

Study region: Brussels (Belgium) and Nantes (France), two cities located in oceanic settings.
Study focus: The article assesses the capabilities of detecting the presence of groundwater in sewers and waste-water in storm sewers (also called parasitic waters), which increase sewer-overflows risk, augment the water-treatment plant operation costs and pollute downstream rivers. This is done by means of Laser Absorption Spectroscopy (LAS) instruments that favor the development of stable isotopes (δ18O and δD) as tracer of urban waters. The study first describes the factors affecting isotopic composition of urban waters. It also describes how to optimize the use of stable isotopes, either alone or coupled with other tracers to detect parasitic waters.
New hydrological insights: In Nantes, groundwater intrusions were detected above 8% of the sewer-water flow and waste-water inflows above 14% of the sewer-water flow. In Brussels, the stable isotopes may trace the presence of parasitic groundwater in a small part of the city territory (9 km^2). This study concludes that stable isotopes can be used as tracer of parasitic waters in low altitude cities close to the ocean, when domestic water originates from catchments extending into the continent. In this case, tracing studies may take advantage of the seasonal variation of the isotopic composition of waste-waters, on the condition of assessing the other factors that impact the isotopic composition of urban waters, as done here.

1. Introduction

1.1. Stable isotopes as tracer

Water stable isotopes ($\delta^{18}O$, δD) have long been used as tracer in hydrological studies in natural catchments and are increasingly used in urban settings (IAEA 2002; Klaus and McDonnell, 2013). The $\delta^{18}O$ and δD values (expressed in ‰) of one particular water-body depend on the physico-chemical processes (e.g. evaporation and condensation) and the climate conditions to which the water-body has been subjected (IAEA, 2000a). Therefore, $\delta^{18}O$ or δD values may be used to qualify and/or quantify the specific climate conditions or the processes that have impacted the different water-bodies (Rozanski, 1985, Schulte et al., 2011) and assess the relative proportion of two or more water sources (also called end-members) in a water-body (Barth and Veizer, 2004; Klaus and McDonnell, 2013). However, their applicability as tracers requires sufficient isotopic differences between end-members (Klaus and McDonnell, 2013). The application of such tracers therefore depends on the correct definition of the isotopic composition of each end-

* Corresponding author.
E-mail address: kevin.de.bondt@vub.be (K. De Bondt).

https://doi.org/10.1016/j.ejrh.2018.06.001
Received 14 October 2017; Received in revised form 1 June 2018; Accepted 2 June 2018
Available online 14 July 2018

member and its variability in both time and space, and often requires numerous samples and analyses.

1.2. Parasitic-waters, an important issue

In this article, $\delta^{18}O$ and δD values are used as tracers in the case of parasitic-waters detection in sewers of Brussels (Belgium) and Nantes (France). Applied to urban areas, the term parasitic water refers to the waters that should not be present in sewers. They may be sorted into four types: 1) groundwater present in combined or sanitary sewers, 2) waste water present in the separate storm sewers, 3) rainwater present in the separate sanitary sewers, 4) domestic waters leaking from supply pipes and entering the combined or sanitary sewers. This paper focuses on the first two types of parasitic waters by estimating the mixing proportion of waste-water and groundwater in sewers.

Parasitic groundwater generally enters sewers (sanitary and combined sewers) through cracks, openings or failures of the sewer walls where the water table level is higher than the invert of sewers (Penckwitt et al., 2016). Groundwater entrances in the sewers can also be caused by direct connections with man-made drains set up to protect house basements and/or to dry up natural resurgences (Weiss et al., 2002; Broadhead et al., 2013). Parasitic groundwater has damaging consequences: i) the limitation of the carrying capacity of the combined sewers and consequently the increase of floods and sewer overflows risks; ii) the augmentation of the volume of water to be treated by Water Treatment Plants (WTP), with as consequence higher operational costs and, through the dilution of the pollutants, the reduction of their removal process efficiency (De Bénédittis and Bertrand-Krajewski, 2005a); iii) the interception of groundwater normally feeding the urban water-courses (Walsh et al., 2012).

Parasitic waste-water mainly enters stormwater sewers through undesirable connections from buildings, from cross connections between stormwater and waste-water sewers or by leakage through failures in the walls of the sewers (Panasiuk et al., 2015). Despite their accidental cause, these undesirable connections constitute a common problem in many cities, which face major difficulties trying to detect and correct these “waste-water inflows” and reduce their negative impacts (Schilperoort, 2004; Irvine et al., 2011). Stormwater sewers are generally not connected to WTP and directly discharge into rivers, ponds and lakes. Therefore, parasitic waste-water, containing nutrients, microbes, pharmaceuticals and endocrine-disrupting compounds constitutes a potential source of pollution for water-bodies. These pollutants are toxic for the water biota, increase the biological oxygen demand, favor the eutrophication of the receiving water-body and represent a human-health issue, if the contaminated water is consumed or even used for recreational purposes (Prüss, 1998; Schwarzenbach et al., 2010; Panasiuk et al., 2015).

Solving parasitic water problems requires detailed knowledge of the waste-water inflows and groundwater intrusions in the whole sewer network. The systematic inspection of all sewers segments represents an enormous task, which demands precautions, manpower, materials and large budgets (Ellis and Butler, 2015). In Strasbourg (France), a budget of more than 2 M€/year is allocated to the rehabilitation program of the sewer system (1600 km length), inculding Close-Circuit Television (CCTV) inspections (Astee, 2015). Kim et al. (2009) indicate CCTV inspection costs around 7,4 USD per meter of sewer and a budget of 12,7 million USD to inspect the sewers of the city of Los Angeles. Moreover the visual inspection of sewers is not able to detect all types of parasitic water entrances (Panasiuk et al., 2015). New scientific methods are thus required to complement, optimize and/or limit sewer investigations in cities (Prigiobbe and Giulianelli, 2009; Staufer et al., 2012). Such methods may aim at two different objectives:

1. “*Quantification*” of parasitic water, either as absolute (i.e. m^3/h) or relative values (e.g.% of the total flow), is generally performed on the main sewers to assess the impact of parasitic waters at the scale of the whole sewer system. It should be exhaustive and provide comparable results for all the parts of the sewer system. The quantification procedure must be representative, by considering either a whole year (or several years) or a period of high inputs (when groundwater table is high, generally during winter and spring). The expected uncertainty should be in the same range as the uncertainty on the flow-rate measurements, around 20% of the assessed absolute value (Bertrand-Krajewski et al., 2000).
2. “*Detection*” aims at providing a presence/absence information of parasitic water, which is useful at the scale of a particular sewer segment to decide whether detailed investigations (i.e. CCTV inspections) should be performed. Detection campaigns performed on a punctual basis and/or over limited periods produce valuable results, as detection of a parasitic water entrance is an important information to decide on the more detailed inspection and/or renovation of sewers. Consequently, representativeness over time, although advisable, is not a strict requirement as in the quantification procedure. Being relatively simple to set-up, the applicability of detection procedures may potentially be compared from one city to another. This paper mainly discusses the detection procedure, which can be achieved by instant grab sampling and isotope ($\delta^{18}O$, δD) analyses.

1.3. Stable isotopes to trace parasitic water presence

Parasitic-water flows are generally quantified based on the daily variation of sewer-water flow-rates (De Bénédittis and Bertrand-Krajewski, 2005a). However, these methods generally overestimate the parasitic-water flows and fail in describing their diurnal variations. In addition to flow-rate measurements, the use of geochemical tracers helps to limit the uncertainty on the calculated volumes of parasitic-water flows (Kracht and Gujer, 2005). These tracers (as salts, ammonia concentration, Chemical Oxygen Demand…) may also be used alone to detect the presence of parasitic water but their application is constrained by the varying composition of wastewater during the day (Kracht and Gujer, 2005; Panasiuk et al., 2015). Artificial tracers (as dye) may be used to detect waste-water inflows but not groundwater infiltrations because of the high chemical background and the turbidity of the wastewater (Penckwitt et al., 2016).

Stable isotopes have numerous advantages and may be used alone or in complement to other tracers and methods to detect

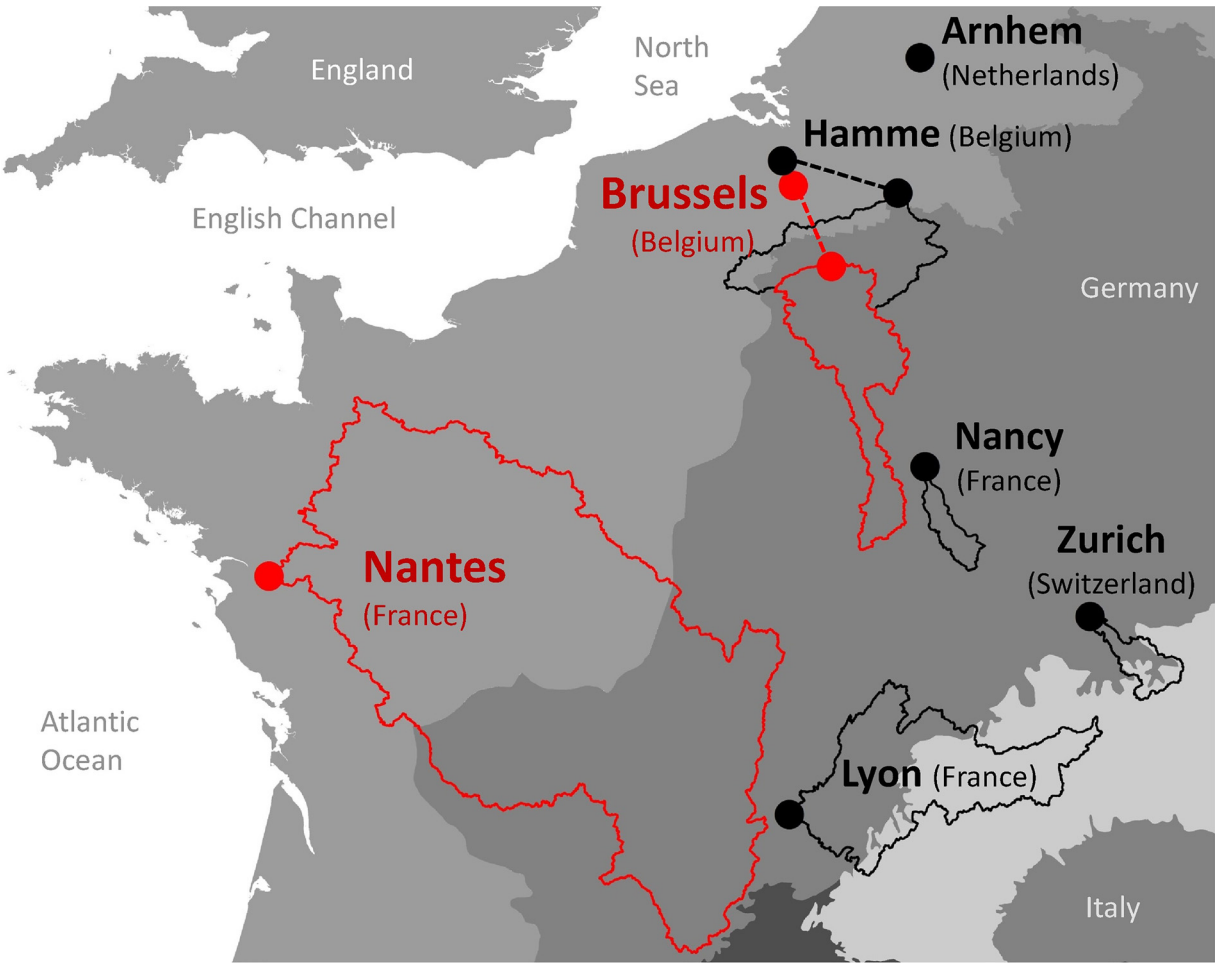

Fig. 1. Cities where the stable isotopes method was successfully applied (in black) and the cities of Nantes and Brussels (in red). The catchment areas influencing the isotopic signal of domestic water are also shown. The background map shows the Bio-geographic Regions (BR) in Europe (European Environment Agency, 2015). From the lightest gray to the darkest gray: Alpine BR, Atlantic BR, Continental BR & Mediterranean BR. (For interpretation of the references to colour in this figure legend, the reader is referred to the web version of this article.)

parasitic waters. One first advantage is that stable isotopes are conservative tracers (Houhou et al., 2010; Klaus et al., 2015): they preserve the original signal of the different parent-water bodies involved in a mixing, independently of chemical reactions, sedimentation, etc. A second advantage is that they are present in every type of water, which is not the case of other geochemical tracers (Almeida et al., 1999) and may detect different types of parasitic-waters (e.g. waste-water and groundwater).

Stable isotopes have previously and successfully been applied to quantify the parasitic-groundwater flows in sewers and Water Treatment Plants (WTP) of Lyon (De Bénédittis and Bertrand-Krajewski, 2005b), Zurich (Kracht et al., 2007) and Nancy (Houhou et al., 2010). In these cities, domestic water is produced from aquifers or surface water in catchments localized in continental climate nearby high mountains (Vosges, Alps, Fig. 1). The high altitude and the lower temperatures affect the isotopic composition of mountain waters (with more depleted $\delta^{18}O$ and δD values). Therefore, the domestic water derived from high-altitude water sources present a more depleted isotopic composition ($\delta^{18}O$ and δD) when compared with the shallow groundwater present under the cities. Moreover, in continental climate, large differences of temperature between summer and winter usually induce a modification of the isotopic composition of the rainwater and surface waters (with less depleted $\delta^{18}O$ and δD values in summer). This variation of $\delta^{18}O$ and δD value during the year is called seasonality effect (IAEA, 2000b). These combined effects (altitude and seasonality) can differentiate the isotopic composition of groundwater and domestic water, up to 3,4‰ $\delta^{18}O$ in Lyon and 12,5‰ δD in Zurich (De Bénédittis and Bertrand-Krajewski, 2005b; Kracht et al., 2007).

Other studies tried to apply this method in oceanic climates with moderate success (Schilperoort, 2004; Schilperoort et al., 2007; Dirckx et al., 2009). The reason is that in oceanic regions, the different water bodies involved present less isotopic variability because of insufficient differences in seasonal temperatures and limited topography effect. Consequently, these studies faced difficulties finding sufficient differences in the isotopic composition between groundwater and domestic water to properly apply the tracing methodology. Among the 7 cases examined in these studies, only two provided satisfactory results. There were carried out in Arnhem in the Netherlands (Schilperoort et al., 2007) and in Hamme in Belgium (Dirckx et al., 2009) (Fig. 1). In these cities, the applications

were succesfull because the $\delta^{18}O$ distinctiveness between groundwater and domestic-water reached 2,25‰ and 1,4‰ respectively. However the end-members were not sufficiently characterized to understand if the method was applicable for the whole city or for a restricted area.

Among all the case-studies examined, both successful and unsuccessful, limiting factors have been pointed out, such as the heterogeneity of the isotopic composition of the infiltrating groundwater, the variability of the domestic-water composition along the year, the complexity of the domestic-water network. However, these studies did not assess separately each factor, and consequently their results are difficult to compare. The potential of stable isotopes methods to localize (and quantify) parasitic water in oceanic cities remains thus uncertain and difficult to assess with respect to the available literature.

Overall, the current literature presents gaps on the use of stable isotopes to trace parasitic waters. For instance, when first proposed (more than 10 years ago), stable isotopes methods were constrained by limited analytical capacities. Today, thanks to Laser Absorption Spectroscopy (LAS) instruments, isotopic studies can be based on a large number of samples to better characterize the composition of the end-members and its variation in time and space (Berman et al., 2009; van Geldern and Barth, 2012). Past studies (in continental and oceanic climates) also commonly used only one water isotope to quantify parasitic groundwater. Now that $\delta^{18}O$ and δD are simultaneously analyzed with the same LAS instrument at higher frequency and with smaller sample volumes, it is possible to test both tracers ($\delta^{18}O$ and δD) on the same samples. Finally, past studies considered that domestic water and waste water have the same isotopic composition because the differences found were weak in comparison to analytical uncertainty (Schilperoort, 2004). The increased precision of the new laser instruments for δD and the possible higher frequency of measurement, allow us to detect small isotopic differences between the different urban-waters.

1.4. Objectives

While existing literature principally detailed the method and its adaptation with post-treatment or complementary tracers, this study emphasizes the determination of the end-members isotopic composition. The objective of this study is to highlight the necessary work to obtain a reliable idea of the potential of stable isotopes as tracer of parasitic water for a city and to give the main keys to optimize the use of stable isotopes as tracers. This article also aims at filling the gaps in current knowledge that can be summarized by the 4 following questions: (1) What is the influence of seasonality on the applicability of the method in oceanic settings? (2) What is the impact of end-member isotopic variability on the method? (3) Is the isotopic composition of waste water the same as that of domestic water? (4) What are the benefits of using two isotopes measured with reduced analytical uncertainty?

To answer these questions, we consider the cases of Nantes and Brussels, two cities presenting, a priori, unfavorable conditions for stable isotopic methods because of their oceanic climate and low altitude. However, part of the domestic water in these two cities is produced from river water with catchments extending further in the continent (Fig. 1). The domestic water thus potentially presents a seasonality effect that may favor the application of stable isotopes as tracers of parasitic waters. The comparison of the two case studies, presenting different environmental conditions and water infrastructure, highlights the general factors determining the potential of stable isotopes for the detection of parasitic waters in oceanic cities and gives the tools to optimize the sampling campaigns.

2. Case-studies

2.1. Brussels

Brussels area (161 km^2) is centered on the Senne Valley, in a relatively flat setting with local hills and valleys, ranging from ~15 m near the river to ~110 m in the heights located mainly to the East, Southeast and to a lesser extent to the Northwest of the city. It is located about 110 km east of the North Sea coast. Here we consider the potential use of stable isotopes to trace the entrance of groundwater from the “Brussels Sands aquifer system” and “the Ypresian hills aquifer system” (Brussels Environment, 2011) into the combined sewer system. In the Brussels Sands aquifer system, the water-table depth ranges from few meters below the surface in the bottom of valleys to more than 30 m in the middle of the highest hills (Dam et al., 1986). The Brussels sands aquifer largely extends on the eastern bank of the Senne (55% of the Brussels area). The intrusion of groundwater into the combined sewers potentially occurs only in limited geographic areas, where the topographical surface cuts the base of the sandy aquifer, underlined by impermeable clay (Buffel and Matthijs, 2008). A similar scenario is present in the valley where the water table is near the surface. The Ypresian hills aquifer system is composed of alternating sand and clay layers of 5–10 m in thickness. This aquifer presents about twenty springs feeding ponds and streams which are connected to the sewer system downstream. These springs, visible in public parks and green zones, are located at different altitudes because of the presence of clay layers and small perched aquifers. This complex aquifer system is present in the North-West of Brussels and covers about 13% of the Brussels area (Brussels Environment, 2011).

For the most impacted sewers in Brussels, the parasitic groundwater may represent up to 77% of the total volume of water (Brussels Environment, 2011) because, during urbanization, most streams and small rivers were incorporated or redirected into the sewer network (Mahaut et al., 2011). The sources of these rivers remain connected to the sewers and probably contribute large volumes of parasitic water. In addition, groundwater also infiltrates through cracks and permeable joints of the old sewers (Brussels Environment, 2011). The relative contribution and the localization of these two types of entrance of parasitic waters (springs and deteriorated pipes) are unknown. However, this information is fundamental for a sustainable management of Brussels' waters.

For the production of domestic water in Brussels, local groundwater is extracted from the Brussels Sands aquifer with 7 wells and 1 underground gallery, providing only 2% of the Brussels' water supply. Most groundwater is extracted outside Brussels from natural

springs, wells, quarry lakes, and underground galleries in 17 production sites localized up to 80 km away from Brussels. Water from the Meuse River is pumped 50 km south-east of Brussels (in Profondeville) and provides nowaday about 30% of the city's water supply (Vivaqua, 2012). The Meuse catchment, upstream of the production plant, extends southward to the Meuse spring localized 350 km from Brussels (Fig. 1). In Brussels, water from the different production plants is mixed in varying proportions as a function of the season, the maintenance works, the consumption, and the reselling to other distribution companies in Belgium (Dirckx et al., 2009). Brussels domestic water is therefore composed of a variable mix of Meuse-river water and groundwater.

2.2. Nantes

Located at the confluence of the Loire, the Erdre and the Sevre Rivers, 55 km far from the Atlantic coast, the city of Nantes has a gentle topography with an altitude varying between 5 and 80 m a.s.l. The city territory (65,2 km^2) extends onto the major bed of the Loire and onto a plateau, composed of bedrock with superficial deposits, notched by small valleys. Given the geology, two types of shallow aquifers can be found: the plateau aquifers (eolian silt over weathered bedrock) and the alluvial aquifers. Here we consider the aquifers in the plateau area, which is located on the northern bank of the Loire and covers 67% of the city territory. In most of the area, the groundwater depth is within 5 m below the surface. In many locations within the Nantes underground, groundwater infiltrates into the sewers, reducing the carrying capacity of the stormwater network and increasing the volume of water treated in WTP of Nantes (Belhadj et al., 1995). Half of the city area, mainly the city center, is equipped with combined sewers, while separate sewers extend underneath the other half. Domestic water in the city of Nantes is exclusively produced from the Loire river, pumped 15 km upstream of the city center.

This study details a sampling campaign that occurred in the "Pin-sec" neighborhood localized in the East of Nantes, whose surface area is 31 ha. In this area, the separate sewer network is composed of a 7,3 km waste water sewer and a 4 km stormwater sewer. The Pin-sec sector is the hydrological catchment defined by the outlet of the stormwater sewer. This catchment has a mean altitude of 22 m asl, and a mean slope of 0,9%. Two geological configurations are present in this area: 1) silt over locally weathered mica-schist is predominant on the upstream part of the neighborhood, and 2) alluvial deposits are located downstream in the valley of the Gohards Stream, to which the stormwater sewer is connected. The water table is between 1 and 2,5 m deep in winter and 3–4 m deep in summer (Le Delliou et al., 2009).

3. Methods

3.1. The mixing-line method

During dry periods the water flowing into the sewers is composed of a mix of groundwater and waste water. As showed by De Bénédittis and Bertrand-Krajewski (2005b), the mixing line method applied with stable isotopes (either $\delta^{18}O$ or δD), estimates a dimensionless proportion of a component (e.g. groundwater) in a compound (waste water + groundwater). For an absolute assessment (e.g. flow or volumes) complementary discharge information must be added to the obtained proportion estimation. The mixing-line method, as developed by De Bénédittis and Bertrand-Krajewski (2005b), can only be applied if there are two distinct end-members (e.g. waste water and groundwater) contributing to the mixing of waters in sewers. If the end-members are unknown and/or if there are more than 2 end-members, other methods such as the "End-Member Mixing Analysis" (EMMA) should be used (Christophersen et al., 1990; Liu et al., 2008; Burns et al., 2001; Vazquez-Sune et al., 2010). The EMMA method has the advantage of integrating multiple tracers, which could be specific of the local groundwater and of the domestic uses. It could therefore be applied to detect parasitic waters in sewers. However, the results are dependent of the type and the number of tracers, and therefore could be difficult to compare between case-studies (Barthold et al., 2011). To reveal the capabilities and the specificities of the stable isotopes as tracer, we decided to apply the mixing-line method with stable isotopes only.

The proportion of parasitic groundwater (P) in the sample is calculated with Eq. (1). If $\delta^{18}O$ is used as tracer, then A and B are calculated with the Eqs. (2a) and (3a). If δD is used, one should refer to the Eqs. (2b) and (3b). To estimate the proportion of waste-water inflows, the terms A&B must be inverted in the Eq. (1).

$$P = \frac{100A}{A + B} \tag{1}$$

$$A = \delta^{18}O_{mix} - \delta^{18}O_{ww} \tag{2a}$$

$$A = \delta D_{mix} - \delta D_{WW} \tag{2b}$$

$$B = \delta^{18}O_{GW} - \delta^{18}O_{mix} \tag{3a}$$

$$B = \delta D_{GW} - \delta D_{mix} \tag{3b}$$

Where P is the he proportion of parasitic groundwater (%), A is the distance (in ‰) between the measured sample on the mixing-line ($\delta^{18}O_{mix}$ or δD_{mix}) and the waste-water end-member ($\delta^{18}O_{WW}$ or δD_{WW}), and B is the distance (in ‰) between the groundwater end-member ($\delta^{18}O_{GW}$ or δD_{GW}) and the same sample ($\delta^{18}O_{mix}$ or δD_{mix})

3.2. Uncertainty on the proportion of parasitic water

The suitability of the mixing-line method for the detection of parasitic water depends on the uncertainty of the proportion estimation. Eq. (4) expresses the uncertainty on P (σP) obtained by propagating uncertainty on the Eqs. (1)–(3) (JCGM, 2008). The σP depends on the analytical uncertainty of the measurement realized on the sewer water sample (σ_{mix}), on the uncertainty associated to the mean isotopic composition of the end-members (σ_{GW} and σ_{WW}), on the distance between the end-members (A + B) and on the position of the sample on the mixing line (A and B). σ_{mix} corresponds to the analytical uncertainty on one measurement. σ_{GW} and σ_{WW} integrate the analytical uncertainty but also the spatial and temporal variability of the end-members, calculated on analyses of many samples. The analytical uncertainty is commonly one order of magnitude smaller than the variability of the end-members. In this case, the analytical uncertainty could be neglected for the calculation of the end-member uncertainty.

$$\sigma P = \frac{100}{(A+B)^2}\sqrt{B^2(\sigma_{mix}^2 + \sigma_{WW}^2) + A^2(\sigma_{mix}^2 + \sigma_{GW}^2)} \tag{4}$$

Where σP (%) is the uncertainty on P, σ_{mix} (in ‰) is the analytical uncertainty of the measurement realized on the sewer water sample, σ_{GW} (in ‰) is the uncertainty associated to the mean isotopic composition of the groundwater end-member, σ_{WW} (in ‰) is the uncertainty associated to the mean isotopic composition of the waste-water end-members.

P may be calculated using either $\delta^{18}O$ (P_{18O}) or δD (P_D) measurements but the two tracers may be also coupled to reduce the uncertainty on the calculated proportion. In this case, P_m is the mean of P_{18O} and P_D, and σP_m is calculated with the Eq. (5):

$$\sigma P_m = \frac{\sqrt{\sigma^2 P_{18O} + \sigma^2 P_D}}{2} \tag{5}$$

Where σP_{18O} (%) is the uncertainty on P calculated with $\delta^{18}O$, σP_D (%) is the uncertainty on P calculated with δD, and σP_m (%) is the uncertainty on P calculated with $\delta^{18}O$ and δD.

Eq. (5), without a covariance term, is valid only if $\delta^{18}O$ or δD are independent tracers (JCGM, 2008). However, measuring $\delta^{18}O$ and δD simultaneously with the same instrument on a single sample may introduce an analytical correlation between $\delta^{18}O$ and δD. Indeed, the absorption peak of the abundant isotopologue ($H_2{}^{16}O$) is used to calculate both $\delta^{18}O$ and δD values. Moreover, the experimental conditions may affect similarly the measurements of the two isotopes. This analytical correlation has been assessed through control measurements that were realized on the same sample between November 2013 and February 2017 (121 measurements, cf. Table A1 in Appendix A). The correlation coefficient found is weak (r^2 = 0,4) and it has been verified that the covariance (cov = 0.004) is negligible in comparison with the terms of Eq. (5) for all the results presented here.

3.3. Detection threshold of the isotopic mixing-line method

The sources of uncertainty in Eq. (5) are the factors limiting the stable isotopes mixing-line method already pointed out before, in this study and in the literature (De Benedittis and Bertrand-Krajewski, 2005b; Schilperoort, 2004). Therefore, the uncertainty on parasitic water proportion (σP), could potentially be used as indicator of the applicability of the mixing-line method. However, σP, calculated on one single sample (Eq. (4)), depends on the mixing proportions and therefore varies from one sample to another. So, we define another indicator to synthesize the combined effect of all sources of uncertainty, that we call the "detection threshold" (P_0). P_0 is the smallest value of P that indicates the presence of parasitic water with a confidence level of 95%. Under the assumption of normal distribution of P, P_0 is the smallest value of P higher than 2σP. If the value of P measured for a sample is equal or higher than P_0, for one tracer or for the average (Eq. (5)), parasitic water is detected in the sample (Fig. 2). The concept of detection threshold is similar to the limit of detection (LOD) defined for analytical methods (JCGM, 2012), but the value of P_0 also takes into account factors of uncertainty as the spatial and/or temporal variability of the two end-members.

As the isotopic composition of the two end-members is rarely homogeneous and constant over entire cities, P_0 varies with time

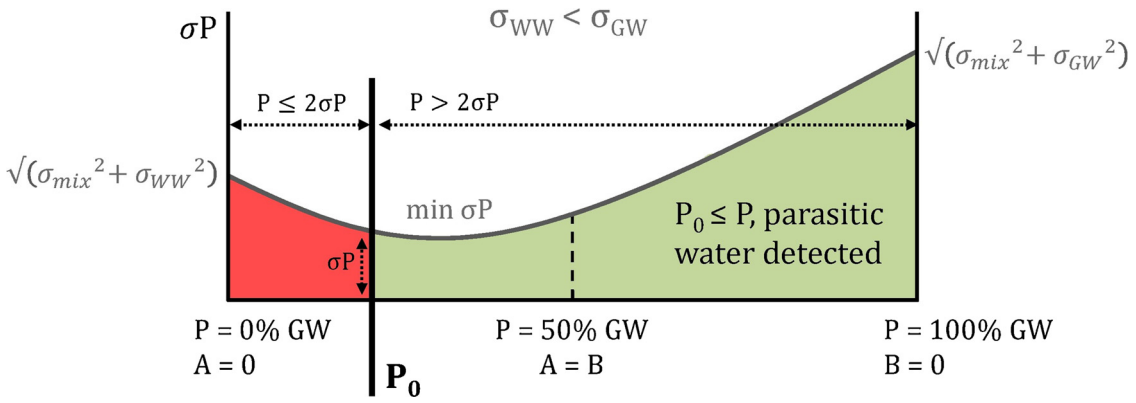

Fig. 2. The concept of "detection threshold" (P_0).

and from one part of the city to another. In this study, we determine and compare the lowest P_0 available in Brussels and Nantes over periods of 2–3 months. The duration is pragmatically selected as the time required to include a sufficient number of dry days to organize sewer sampling campaigns. Indeed, parasitic water detection using stable isotopes requires the organization of multiple sampling campaigns to reach more precise results (see further) and to explore the numerous sewer segments potentially impacted by parasitic water.

3.4. Sampling and analyses

A total of 265 water samples were collected during the period October 2010–September 2014 in glass or high density polyethylene bottles, hermetically sealed with caps dedicated for long-time storage and with paraffin film. The bottles were stored in the dark at 4 °C before analyses at the Vrije Universiteit Brussels stable isotopes laboratory. We performed replication tests that showed that storage time did not affect the quality of the results. Groundwater was sampled in natural springs or in groundwater pumping stations and observation wells, after the water in pipes and wells, potentially in contact with air, was totally purged. The domestic water was collected in household taps located within the investigated parts of the cities, once or twice a month, also after purging the water already present in pipes. The waste-water was manually collected in manholes and segments of sewers in the morning (8A.M.–1P.M.) in both case-studies. Rainwater was collected in samplers that automatically close after the rain event to avoid fractionation of the isotopic composition due to evaporation. Groundwater, rainwater and waste-water samples were filtered at 0,2 μm via syringe filters before analysis using a Laser Absorption Spectroscopy (LAS) instrument (Picarro L2130-i).

The LAS instruments make isotopic analysis relatively robust, fast and low cost. LAS instruments determine the isotopic composition of water by measuring the energy absorption (in the near infra-red range) by the rotational-vibrational transitions in three isotopologues ($H_2{}^{18}O$, $H_2{}^{16}O$ and $HD^{16}O$) of the water molecule (van Geldern and Barth, 2012). However, LAS measurements are vulnerable to dissolved organic carbon, methane and methanol present in water, which may interfere with the absorption spectrum of the water vapor and could affect the calculation of the isotope ratios (Brand et al., 2009). This bias was reported for isotopic analyses of water extracted from plants and soils (West et al., 2010; Martin-Gomez et al., 2015) but could potentially be also present in river or waste waters (Singleton et al., 2009). Therefore, we conducted a test by comparing isotopic analyses of waste water and domestic water with the Picarro L-2130i (in different configurations) and withIsotope-Ratio Mass Spectrometer (cf. Table B1 in Appendix B). The different configurations of the Picarro L-2130i depend on the carrying gas: N2 or dry air. In the second configuration, the absorption peak of water isotopes is automatically corrected if methane or methanol is present, while in the first configuration no correction was performed (Picarro, personal communication). When using IRMS, the water isotopic composition is not modified by dissolved organic carbon, methanol and or methane (West et al., 2010). The drinking waters are taken as reference as they typically contain very low concentration in dissolved organic carbon, methane and methanol. The results of the test show no effect due to the possible presence of these components, as the isotopic composition of waste water are identical for IRMS and LAS analyses.

The LAS instrument are typically affected by a “memory effect” which is a shift in the isotopic value of the sample due to traces of the preceding sample in the current analysis. To lower the impact of the memory effect, we adapted the experimental protocols during the study. The best option found is to calculate a memory effect ratio by parts of the experiment and then correct it, following the procedure described by IAEA and USGS (2013). Moreover, we injected the samples 6–7 times but we calculated the mean $\delta^{18}O$ and δD values on the last 3 injections only. The resulting analytical uncertainty with the LAS instrument at the AMGC laboratory is 0,06‰ for $\delta^{18}O$ and 0,3‰ for δD (2σ). This typical analytical uncertainty is calculated on replicates of control house standard randomly placed between samples in different experiments and constitutes an improvement in comparison with uncertainties of analyses reported in previous studies, which were, at best, 0,1‰ for $\delta^{18}O$ and 1‰ for δD (2σ) (De Bénédittis and Bertrand-Krajewski, 2005b; Houhou et al., 2010).

4. Results

This section details the post-treatment steps of the isotopic results to characterize the mean isotopic composition of the end-members, to obtain significant detection thresholds for both cities and to test the method in situ. Table 1 reports the mean isotopic data (and the standard-deviation) for all water types analyzed during this study. The individual analyses are reported in the Table C1 in Appendix C.

4.1. Groundwater end-members

The characterization of the isotopic composition of groundwater represents an important step to assess the potential of the method to detect parasitic water. It defines the uncertainty of one end-member and partly determines the length of the mixing-line. In Nantes, groundwater from plateau aquifers was sampled in two locations distant of 15 km from each other, in the west part (Chézine) and in the eastern part (Pin-sec) of Nantes (Table 1). The sampling stations show isotopic compositions constant through seasons (and from one year to another) within the range of −5,58 to −5,26‰ for $\delta^{18}O$ and −35,8 to −32,2‰ for δD (cf. Table C1 in Appendix C). The groundwater from these two locations is considered as a single GW end-member with a mean isotopic composition of −5,43‰ & −33,8‰ and a variability (σ) of 0,10‰ & 1,2‰, for $\delta^{18}O$ and δD respectively.

In Brussels, two aquifers were sampled: The “Ypresian hills aquifer system” (North-West) and the “Brussels Sands aquifer system” (East of Brussels). The results in Table 1 shows that both aquifers have a similar mean isotopic composition but different seasonal variability. This observed isotopic variability is mainly explained by the resurgence of “Ypresian hills” groundwater into springs,

Table 1
Mean isotopic signal and standard deviation (σ) of the different waters analyzed for Brussels and Nantes. GW = groundwater.

Type of water	n° of stations	n° of samples	period of sampling	$\delta^{18}O$ (‰)	σ $\delta^{18}O$ (‰)	δD (‰)	σ δD (‰)
Brussels (180 samples)							
GW « Brussels Sands » aquifer (under urban settings)	15	40	Sept 2011–Dec-12	−7,18	0,11	-47,9	0,5
GW « Ypresian hills » aquifer (wells & springs)	9	47	Nov. 2010–Dec. 2012	−6,95	0,24	-45,7	1,5
Domestic water, Meuse water only	1	56	Aug. 2010–Oct. 2012	−7,05	0,42	-46,9	2,5
Domestic water, campaigns “Waste-water shift”	8	9	July 2012, Sept. 2013 & Sept 2014	−7,17	0,17	-47,4	1,0
Waste water, campaigns “Waste-water shift	24	28	July 2012, Sept. 2013 & Sept 2014	−7,02	0,11	-46,5	0,3
Nantes (85 samples)							
GW West of Nantes (Chézine)	3	6	Febr. & June 2013	−5,42	0,12	-32,4	0,3
GW East of Nantes (Pin-sec)	5	26	Febr.–Aug. 2013 & March–June 2014	−5,43	0,10	-34,2	1,0
Domestic water, Loire water only	1	22	Oct. 2012–Jun-14	−6,15	0,61	-41,9	2,8
Detection campaigns, sewer water (Pin-sec)	17	31	May 2013 & Mar-14	−6,21	0,66	-39,9	5,1

streams and ponds, which are connected to the sewers. These open-air water-bodies are subject to evaporation that enriches their isotopic compositions in heavy isotopes. The enrichment varies according to the season (stronger in summer), the micro-climate conditions (temperature, air moisture) and the residence time of the water at open air (De Bondt and Claeys, 2015). Open-air streams and ponds collected into the sewers largely contribute to the parasitic water flows and lead to a higher uncertainty on the isotopic value of the Ypresian hills aquifer in summer. The “Brussels sands” aquifer is covered by urban settings and by the Sonian Forest. In the forested part, many natural springs feed ponds and streams but these water-bodies are connected to water-courses and not to the sewers. In the urban part, ponds and streams have generally been drained and covered. Therefore, the groundwater infiltrates the sewers in the underground without being affected by evaporation. The Brussels sands aquifer (under urban settings) presents an isotopic composition that is geographically homogeneous and remains stable through the seasons and the years around the mean isotopic composition of −7,18‰ for and −47,9‰ for $\delta^{18}O$ and δD respectively (Table 1; Table C1 in Appendix C; De Bondt and Claeys, 2015).

The large seasonal variability of the isotopic composition of Ypresian hills end-member (Table 1) is a potential source of uncertainty for the mixing-line method. Looking for the best situation possible, we limit the application of the mixing-line method to parts of the territory where the Brussels sands aquifer is the GW end-member. It is interesting to note that the distinction between these two aquifers is not only based on their different geological characteristics but is also (and mainly) related to the type of parasitic groundwater intrusion (open-air streams or underground leakage).

4.2. Waste-water end-members

Previous studies often considered the waste water and domestic-water isotopic composition to be identical (De Bénédittis and Bertrand-Krajewski, 2005b; Kracht et al., 2007; Houhou et al., 2010). However, Schilperoort (2004) studied the fractionation processes occurring during domestic use and assessed separately the effect of various water usages (bath, shower, toilet, cooking) and the addition of urine on the isotopic composition of domestic water. When combined, these effects induce an enrichment in heavy isotopes of ~0,12‰ for $\delta^{18}O$. This enrichment value is calculated on a daily mean and undoubtedly can change during the day depending on the domestic-water use (Almeida et al., 1999). The varying fractionations increase the uncertainty on the isotopic signal of waste water and should therefore be further characterized.

To characterize the possible enrichment, we compared the isotopic composition of waste- and domestic-waters from the same areas (Fig. 3). The sampling sites were carefully chosen to collect only waste water. At these locations, the local groundwater is situated below the base of the sewer pipes in the underground. The waste-water samples were exclusively collected in dry periods (more than 48 h after rain events). In all the sampling campaigns, we note a systematic enrichment in heavier isotopes of waste water compared to domestic water. The shift in Brussels is of 0,13‰ for $\delta^{18}O$ and 0,7‰ for δD. This enrichment presents a mean slope of ~5.2 on a $\delta D/\delta^{18}O$ diagram that may indicate a partial evaporation (IAEA, 2000b) and supports the hypothesis that the usage of domestic water for bath, shower, and cooking, in combination with the presence of urine, causes the enrichment of the waste water in heavy isotopes. In Nantes, undiluted waste-water was collected in May 2013 and March 2014 in the sewer of a collective housing building. Here as well, the isotopic composition of the waste-water was enriched, by 0,14‰ and 1,0‰ for $\delta^{18}O$ and δD respectively, when compared to tap-water collected the same day.

We therefore consider the waste-water end-member signal to be equal to the isotopic composition of domestic water plus a mean enrichment of 0,13‰ for $\delta^{18}O$ and 0,8‰ for δD. This shift is valid for both cities but for the morning only, as the domestic water use may induce other enrichment for other periods of the day. It is interesting to note that the sampling-campaigns occurred in the summer. Therefore, condensing boilers, which may also cause a strong fractionation of the domestic water signal (Schilperoort, 2004), were most likely not contributing to this enrichment. The enrichment shift calculated for Nantes and Brussels may therefore also vary according to the seasons and should be characterized before organizing detection campaigns.

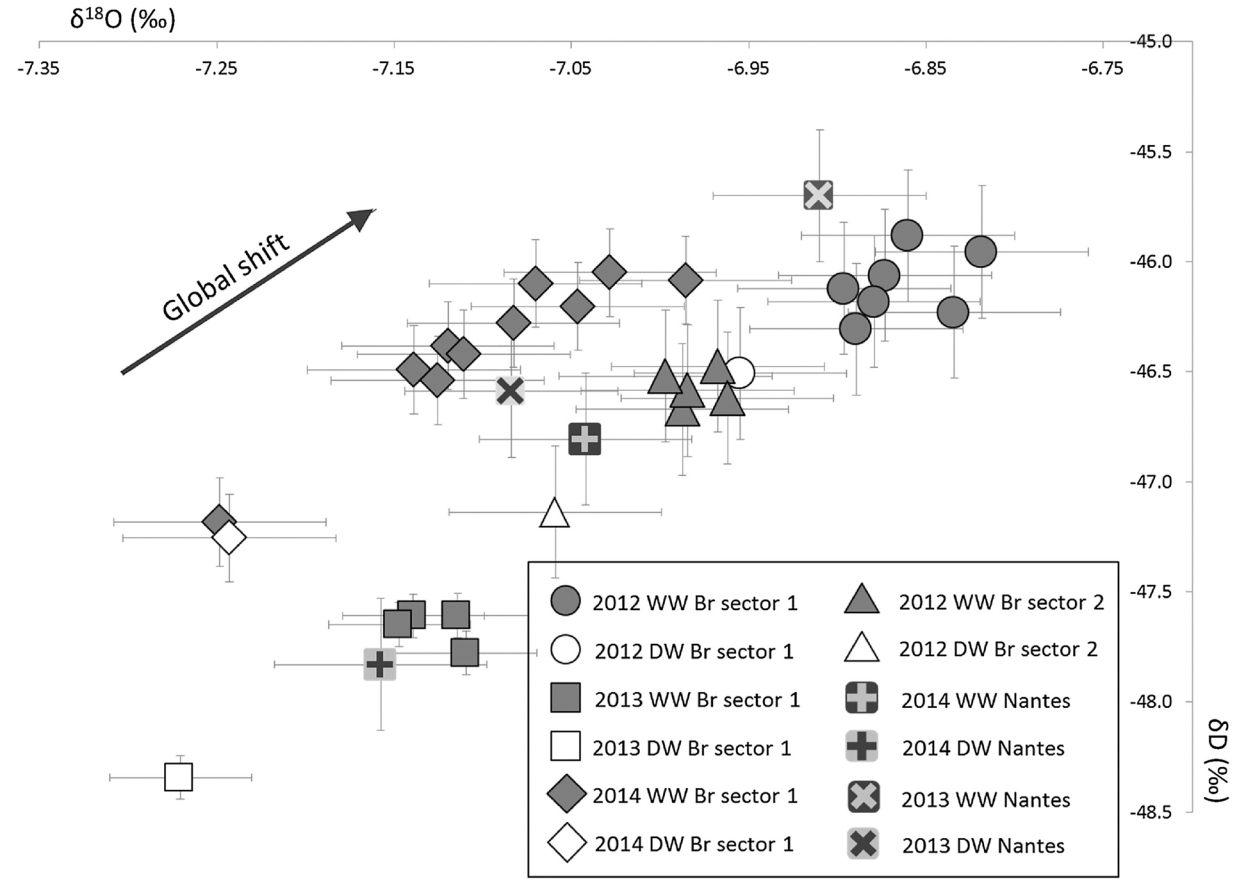

Fig. 3. Isotopic composition of domestic water (DW) and undiluted waste water (WW), in Nantes and in Brussels (Br).

From the results of these sampling campaigns, we consider, for the rest of the work, the uncertainty (2σ) on the isotopic composition of the waste-water end-member equal to 0,2 for $\delta^{18}O$ and 0,6 for δD.

4.3. Seasonality effect

Domestic waters from rivers are impacted by a seasonality effect that may create sufficient isotopic distance (denominator "A + B" in Eq. (4)) between end-members to identify parasitic waters. To characterize this effect, we organized the regular sampling of the domestic water (once or twice a month) in Nantes and Brussels revealing variation of normalized $\delta^{18}O$ and δD distances through the seasons (Fig. 4).

In Brussels, domestic water from Meuse water is enriched in $\delta^{18}O$ and δD during the late summer (Fig. 4) in comparison with local groundwater, because of the $\delta^{18}O$ and δD rich (hot) summer precipitations (IAEA, 2000b). Such enrichment may also result from stronger evaporation of surface waters. In winter, snow-cover melting from the upper part of the Meuse catchment (~500 m a.s.l.) explains the depleted signatures.

Nantes show a continental effect (IAEA, 2000b) as almost all the Loire water is more depleted in $\delta^{18}O$ and δD than the local groundwater. Moreover, the isotopic composition of the Loire largely varies according to the season. During late winter or spring, $\delta^{18}O$ and δD values are lower (Fig. 4) because of the snow melting upstream of the Loire catchment in the Massif Central (IAEA, 2000b). The late melting period of 2013 is clearly identifiable.

4.4. Detection thresholds

Periods of two to three months with the largest isotopic distance between ground-and domestic- water were identified base on the seasonality effect. In Brussels, optimal conditions for sampling occurred in July-September 2011 and August-September 2012, while,in Nantes, from mid-May to the beginning of August in 2013 and from February to April in 2014. Using Eqs. (5) and (6), the detection thresholds for parasitic groundwater in Brussels are 13% for 2011 and 23% for 2012 (line D in Table 2). Detection thresholds of waste-water inflows have also been calculated even if, in a combined sewer as in Brussels, waste-water is not a parasitic water. In Nantes, the detection thresholds are similar from one year to another with 7 or 8% for parasitic groundwater and 14 or 15%

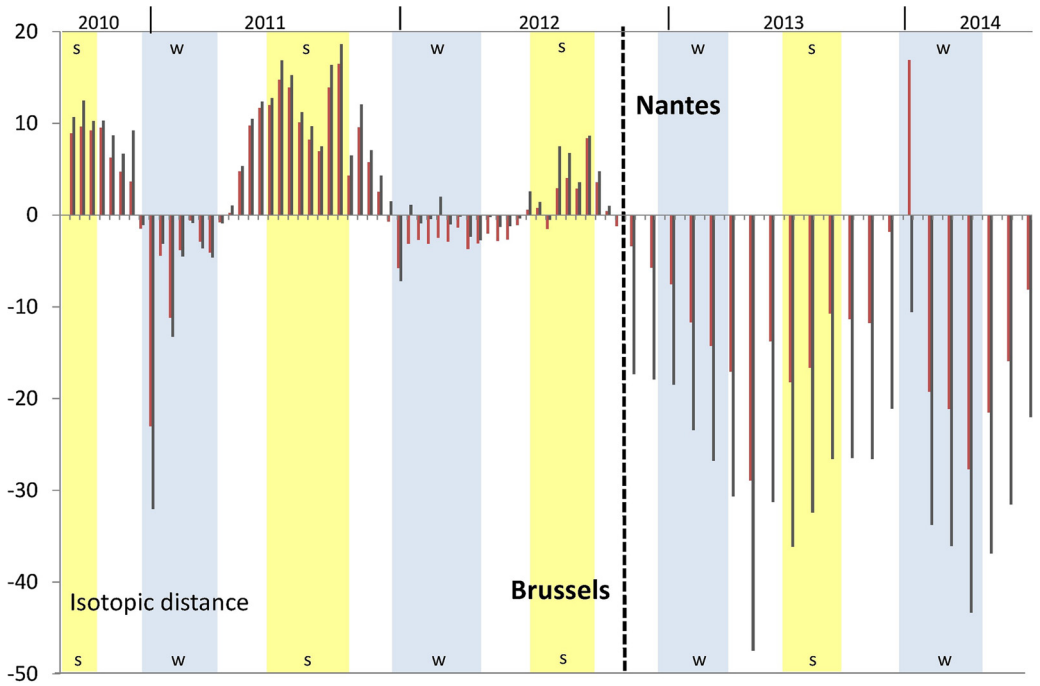

Fig. 4. Isotopic distances between groundwaters and domestic waters, from the 26/08/10 to 30/10/12 in Brussels, and from the 02/10/2012 to the 16/06/14 in Nantes. The $\delta^{18}O$ distances (in red) and δD distances (in grey) are normalized by dividing the distances by the corresponding analytical uncertainty. Negative distances indicate that domestic water is more depleted in heavy isotopes than groundwaters. S and W refer to Summer and Winter respectively. (For interpretation of the references to colour in this figure legend, the reader is referred to the web version of this article.)

Table 2
Detection thresholds for Brussels and Nantes when $\delta^{18}O$ and δD are used separately or coupled (m). The lowest detection threshold for each situation (for each line) is underlined.

	Brussels 2011 (08/07–20/09)		Brussels 2012 (06/08–01/10)		Nantes 2013 (03/04–28/06)		Nantes 2014 (11/02–30/04)	
	$\delta^{18}O$	δD	$\delta^{18}O$	δD	$\delta^{18}O$	δD	$\delta^{18}O$	δD
A. WW isotopic variability (2σ, in ‰)	0,20	0,6	0,20	0,6	0,20	0,6	0,20	0,6
B. GW isotopic variability (2σ, in ‰)	0,22	1,1	0,22	1,1	0,20	2,3	0,20	2,3
C. Distance between end-members (in ‰)	0,85	4,8	0,39	2,6	1,03	9,9	1,21	10,2

	Brussels 2011			Brussels 2012			Nantes 2013			Nantes 2014		
	$P_0{}^{18}O$	P_0D	P_0m	$P_0{}^{18}O$	P_0D	P_0m	$P_0{}^{18}O$	P_0D	P_0m	$P_0{}^{18}O$	P_0D	P_0m
Good analytical uncertainty												
D. Detection threshold GW	21%	13%	13%	41%	23%	25%	18%	8%	11%	16%	7%	9%
E. Detection threshold WW	23%	20%	16%	42%	32%	29%	18%	20%	15%	16%	19%	14%
Common analytical uncertainty												
F. Detection threshold GW	22%	21%	16%	43%	36%	29%	19%	12%	12%	17%	11%	11%
G. Detection threshold WW	23%	25%	19%	44%	40%	32%	19%	21%	15%	17%	21%	14%

for waste-water inflows (lines C & D in Table 2).

The most important difference between Brussels and Nantes, that can explain the difference in the detection thresholds, is the total distance between end-members. A second key parameter influencing the detection thresholds is the isotopic variability of the end-members. As an example, the waste-water detection thresholds of Brussels in 2011 and those of Nantes are similar (line E, Table 2) because of the smaller isotopic variability of the GW end-member in Brussels. In this case, the end-member variability factor is almost as important as the distance factor.

The mixing-line using both $\delta^{18}O$ and δD resulted in lower detection thresholds than those based on one tracer only. Indeed, when

Table 3
Parasitic-water proportion (P) + the detection thresholds (P_0) of the samples collected during the campaigns in the Pin-Sec catchment (Nantes), in May 2013 & March 2014. SW = stormwater, DW = domestic water, GW = groundwater. The sewers underlined present parasitic waters while the outliers cannot be characterized by the mixing-lines. The sewers are sorted based on the proportion of parasitic groundwater (P_{GW}) in the results of the campaign 2013.

Campaigns		May-13			Mar-14		
Sewer segment	Parasitic water	$P^{18}O$ (P_0)	PD (P_0)	Pm (P_0)	$P^{18}O$ (P_0)	PD (P_0)	Pm (P_0)
SW 1tot	WW	−5% (14)	−2% (15)	−3% (11)			
SW 1a	WW				Outlier	Outlier	Outlier
SW 1b	WW				−10% (14)	−10% (16)	−10% (12)
Outlet SW	WW	−1% (14)	3% (15)	1% (11)	−2% (14)	−4% (16)	−3% (12)
SW 2	WW	4% (14)	4% (15)	4% (11)	3% (14)	1% (16)	2% (12)
SW 3	WW	1% (14)	6% (15)	4% (11)	−4% (14)	−1% (16)	−2% (12)
SW 4	WW	29% (14)	31% (15)	30% (11)	0% (14)	−1% (16)	−1% (12)
SW 5	WW	43% (14)	42% (15)	42% (11)	−2% (14)	−2% (16)	−2% (12)
WW 1	GW	42% (12)	40% (5)	41% (7)	53% (13)	53% (6)	53% (8)
WW 2	GW	23% (12)	23% (5)	23% (7)	13% (13)	15% (6)	14% (8)
WW 3	GW	22% (12)	21% (5)	21% (7)	49% (13)	52% (6)	50% (8)
Outlet WW	GW	14% (12)	13% (5)	13% (7)	Outlier	Outlier	Outlier
WW 4	GW	13% (12)	12% (5)	12% (7)	12% (13)	11% (6)	11% (8)
WW 5	GW	10% (12)	11% (5)	10% (7)	7% (13)	6% (6)	6% (8)
WW 6	GW	11% (12)	11% (5)	11% (7)	Outlier	Outlier	Outlier
WW 7	GW	8% (12)	8% (5)	8% (7)	1% (13)	−2% (6)	−1% (8)
WW 8	GW	2% (12)	4% (5)	3% (7)	3% (13)	1% (6)	2% (8)

End-members	May-13		Mar-14	
	$\delta^{18}O$ ($\sigma\delta^{18}O$)	δD ($\sigma\delta D$)	$\delta^{18}O$ ($\sigma\delta^{18}O$)	δD ($\sigma\delta D$)
WW (DW + shift)	−7,04‰ (0,11)	−46,0‰ (1,2)	−6,95‰ (0,11)	−45,8‰ (1,1)
Mean GW	−5,43‰ (0,10)	−32,6‰ (0,3)	−5,44‰ (0,10)	−34,3‰ (0,3)

the detection thresholds with $\delta^{18}O$ and δD are similar, the coupling of the two tracers (through Eq. (5)) lowers the detection threshold of 4%. The small instrumental uncertainty achieved in this study also lowered detection thresholds, particularly in Brussels (up to 13%).

4.5. Detection campaigns in real condition in Nantes

The detection thresholds calculated in the previous section provide valuable information on the potential of the method in both cities. However, to test the method in real conditions, we conducted two detection campaigns in the Pin Sec catchment (Nantes) in May 2013 and March 2014. We collected groundwater in 5 observation wells to characterize the mean groundwater isotopic composition. We also collected 31 samples in the waste water and stormwater sewers between 8 and 12 A.M. The isotopic composition of the waste-water end-member corresponds to the tap-water sample collected the same day plus the isotopic shift. Its uncertainty is that of the waste-water shift. The low detection thresholds (Table 3) are due to the very large and favorable isotopic distances between the end-members (Fig. 4). The campaign of 2013 shows 8 sewer segments with detectable parasitic groundwater and 2 stormwater sewer segments with waste-water inflows (Table 3). These waste-water inflows were not detected at the outlet of the network, neither in the March 2014 campaign, suggesting that waste-water inflows in the stormwater sewers may be very sudden (Panasiuk et al., 2015).

The campaign highlighted also another benefit of the combined use of $\delta^{18}O$ and δD: the possibility to verify that the mixing system is well described, which is a necessary condition to apply the mixing-line method (Houhou et al., 2010; Kracht et al., 2007). The sewer samples are plotted in a $\delta^{18}O/\delta D$ diagram, that traces the mixing-line (Fig. 5) and show that the end-members are well determined as most of the samples fall on the $\delta^{18}O/\delta D$ mixing-line. However, for the March 2014 campaign, the proportions of parasitic water in 3 sewer segments (in red in Table 3) deviate from the mixing-line. Apparently, other sources of water, or local variations of the end-members, contribute to the water volume in these 3 pipes. This is interesting as it points out the sewers affected by complex or specific groundwater intrusions that must be taken into account when adapting the sewer renovation program to the local situation. The mixing line method applied with only one tracer is not able to detect these 3 outlying samples.

5. Discussion

5.1. Applicability of the isotopic mixing-line method in Brussels and Nantes

The detection thresholds in Brussels were 13% of parasitic groundwater in 2011 and 23% in 2012, which allow detection of most groundwater intrusions in 2011, but may limit the potential of detection in 2012. Other factors also lower the applicability of the

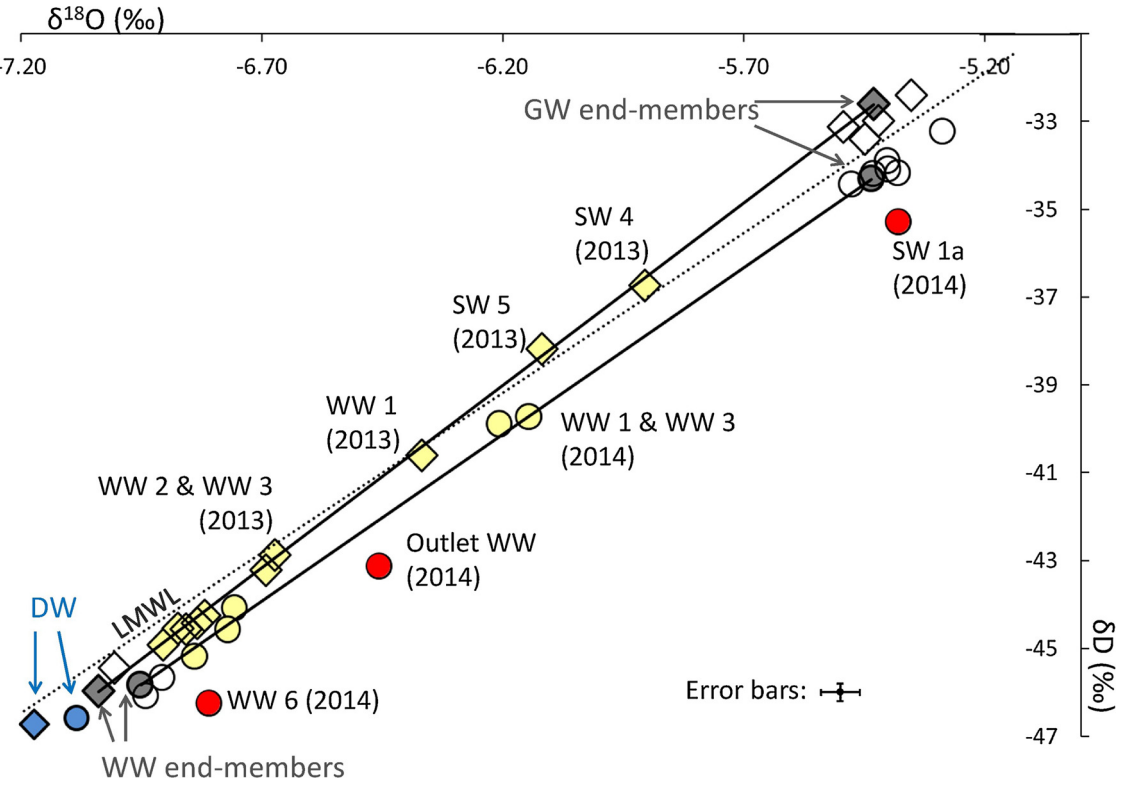

Fig. 5. Isotopic results of the sampling campaigns in Nantes in May 2013 (diamonds) and in March 2014 (circles). Grey represents mean isotopic composition of the end-members. The sewers in yellow show the presence of parasitic waters, those in white do not present any detectable parasitic waters. The samples in red cannot be characterized by these mixing-lines. Domestic waters isotopic compositions are in blue. The numbers refer to the label of sewer segments in Table 3. "WW" and "GW" refer to "waste water" and "groundwater" respectively. The dashed line represents the LMWL based on the analyses of rainwater samples collected in the Chézine and the Pin-Sec sites (see Table D1 in Appendix D). (For interpretation of the references to colour in this figure legend, the reader is referred to the web version of this article.)

stable isotopes method in Brussels. First, the optimal period for applying the isotopic method is summer, when groundwater levels are the lowest and only permanent groundwater intrusions are present (de Ville et al., 2017), making seasonal (winter) intrusions non-detectable Second, a sector of 9 km^2 (6% of the city area), in the South of Brussels, receives Meuse water only as domestic water with potential Brussels sands groundwater intrusions. Therefore, the rest of the city is expected to present higher detection thresholds due to the lack of seasonality effect in waste-water isotopic composition and/or increased uncertainty on the isotopic composition of the end-members (waste-water and groundwater). The city of Brussels should then be divided in homogeneous isotopic sectors each having a determined pair of end-members (groundwater and waste-water). The extension of each sector depends on the local geology, the type of parasitic-water entrance, the water supply sources and their mixing in the water supply system. Sector's extension may thus be highly variable.

This work allows to assess the applicability and the efforts required by the stable isotopes method and show that it is not ideal to detect groundwater intrusions in Brussels. However, in Brussels, the applicability of the method mays benefits from the short-time variation of the isotopic composition of the Meuse water (cf. Fig. 4). A possible strategy could be to regularly monitor the isotopic composition of the domestic-water, in summer and in winter, to organize short sampling campaigns when the conditions are optimal during few days or weeks. With such intense monitoring effort, the stable isotopes method could be applied during the winter to detect seasonnal groundwater intrusions and extended to sectors where Meuse water is mixed with other water supply sources (about 40% of the city area).

In Nantes, the detection threshold are 7–8% of parasitic groundwater, which is sufficient to locate most of the relevant groundwater entrances into the sewer system, at any time of the day. The detection threshold of waste-water is also relatively small (14–15%) and makes the stable isotopes method fully capable of detecting waste-water inflows into the stormwater sewers. These low detection thresholds are caused by a large isotopic difference between Loire water and the groundwater in the plateau aquifers in spring (i.e. the distance between end-members). The periods when the distance between end-members is the largest (snow melting in the Massif Central) may be foreseen weeks in advance. The mixing-line method may also be applied during less optimal seasons, certainly with higher thresholds, but sufficient to determine seasonal groundwater intrusions. Moreover, the domestic-water supply network is simple and does not divide the city into sectors. The only division made in Nantes could be between the plateau aquifers and the alluvial aquifers not assessed in this study.

5.2. Quantification procedures in water treatment plants or sector by sector?

Although this study focuses on the detection of parasitic water presence, lessons can be drawn for the application of a quantification approach with stable isotopes, in combination with flow measurements. With an uncertainty (2σ) on the calculated proportion of less than 10% of the total volume (as in Nantes), the method seems applicable for quantification approaches, eventually by organizing night sampling campaigns, when groundwater flow proportions are higher.

However, it is important to remember that the results from Nantes are valid only for the plateau aquifers. In other areas, alluvial aquifers probably also contribute to the parasitic flows arriving in WTP, increasing the end-members heterogeneity and affecting the distance between the end-members. In general, if multiple sectors contribute to the sewer-water flow, a precise quantification may be difficult to reach in WTP and in large catchments. Conversely, the stable isotope method is facilitated when it is applied sector by sector.

5.3. Practical application of stable isotopes and other tracers in sewers

In this study, we choose to use stable isotopesalone to compare the case studies and to reveal the capabilities but also the limits of the stable isotopes as tracer in sewers. The first limitation concerns the use of stable isotopes as tracers at the city-scale (see before). The second limitation is that stable isotopes are unable to discriminate parasitic waters having similar end-members. As an example, for the sampling campaigns in Nantes, the domestic waters are positioned in the alignment of the mixing-line (Fig. 5) and, in this case, a parasitic domestic-water, leaking from supply pipes, would not deviate the samples from the mixing-line and would not be discriminated from parasitic waste-water. Moreover, the presence of infiltrated rainwater in sewers may or may not lead samples deviating from the mixing-line, depending on the isotopic composition of the rain events, along the LMWL (Fig. 5). The discrimination potential of stable isotopes for all the different types of water is therefore variable and case-specific. If multiple types of parasitic waters are present in the sewers, other tracers should be applied in addition to stable isotopes, as $\delta^{34}S$ or $\delta^{18}O_{SO4}$ (Houhou et al., 2010). If stable isotopes are part of the tracers set, we recommend performing detailed studies, similar to the one proposed here, to asses all the factors influencing the stable isotopes potential. These preliminary studies should cover one year minimum with a sampling campaign once a month or more to assess the seasonality effect and should have as objective to divide the city in isotopic sectors based on the identification of different end-members. The time and resources invested in such preliminary study will be counter-balanced with the benefits for the tracing studies. The evaluation of the potential of stable isotopes as tracer all year long allows to optimize the set of tracers from one season (or period) to another. The division of the city territory in sectors makes it possible to adapt the number and types of tracers from one sector to another and to reduce the uncertainty on the isotopic composition of end-members. This optimization process would improve the results (whatever the mixing method used) and may reduce analytical or sampling cost/time of the tracing studies. These benefits will be particularly valuable in the framework of a continuous monitoring of the sewer system. The continuous monitoring aims at increasing and updating knowledge on the system to improve the sewer renovation program and assess the impact of this last. Such monitoring program is receiving increasing attention. For example, continuous monitoring of sewers is now prescribed by French regulations (Joannis et al., 2015). In this case, the initial investments in time and resources decrease for continuous monitoring based on multiple years.

6. Conclusions and perspectives

The first objective of this work was to assess the potential of the mixing-line method with stable isotopes to trace parasitic waters in cities close to ocean. To get an overall indicator of applicability, we proposed to calculate “detection thresholds” in different conditions in Nantes and Brussels. In Nantes, the stable isotopes are applicable to detect groundwater intrusions (above 8% of the sewer flow) of and waste-water inflows (above 14% of the sewer flow) for the whole plateau area. In Brussels the applicability of the method is limited as it strongly varies from one year to another. Moreover, its applicability is demonstrated over only 6% of the city and the methode requires intense efforts to monitor the variability in time of the end-members for the rest of the city.

This study also assessed the individual factors determining the applicability of stable isotopes. By comparing the detection thresholds for different conditions with the real sampling campaigns, we answer the question derived from the current literature and raised in the introduction.

1) *What is the influence of the seasonality on the applicability of the method in oceanic settings?*

If issued from rivers, domestic water, and thus waste water, shows a seasonality effect that may vary across years (in intensity, in duration and in period) making it difficult to define a priori. In our case-studies, the seasonality effect has a major impact on the applicability of the method.

2) *What is the impact of the variability of the isotopic composition of the end-members?*

End-members variability has a determining impact on the applicability of the mixing-line method, especially for cities where the isotopic distance is small, as in Brussels. Dividing cities into homogeneous isotopic sectors based on the geology, the type of connection with the sewers and the water supply network structure is a strategy that can help to reduce this impact.

3) *Is the isotopic composition of waste water the same as than that of domestic water?*

No. The isotopic composition of pure waste-water, collected in sewers of Nantes and Brussels, is enriched in heavy isotopes with respect to the domestic water due to the household uses.

4) *What are the benefits of using two isotopes measured with reduced analytical uncertainty?*

Here, the application of the mixing-line method with both $\delta^{18}O$ and δD (measured with good analytical uncertainty) resulted in detection thresholds of parasitic groundwater reduced of 20% in Brussels and of 11% in Nantes, in comparison with the application of the mixing-line with $\delta^{18}O$ measured with common analytical uncertainty. Identification of mixing anomalies in the sewers, as the three outlyers samples in the Pin-sec campiagns, is a secondary benefit.

Thanks to the development of the LAS instrument, stable isotopes may become common tracers of urban-water bodies. Using stable isotopes requires a precise understanding of all the factors determining their efficiency. Therefore, the focus on stable isotopes in this article together with the work on the seasonality effect, on the isotopic sectors and on detection thresholds, shows how to perform optimized mixing-studies. This benefits to the application of the mixing-line method to detect parasitic waters in oceanic cities but could also favor studies with other objectives and/or under different climate. This optimization process could also benefit to mixing studies with stables isotopes coupled with other tracers. This should be tested and constitutes an interesting perspective of work.

Conflict of interest

None.

Acknowledgements

The authors thank Brussels Environment and Vivaqua staff members, Katia Chancibault and Laetitia Pineau (IFSTTAR) for their contribution to the water sampling in Brussels and Nantes, and also H. Meijer for his contribution to the improvement of the article. This work received the financial supports of the National Institute for Earth Sciences and Astronomy (INSU) of the Centre National de la Recherche Scientifique (CNRS) (EC2CO Rosenhy), the Brussels-Capital Region (Innoviris) and the Region Pays de la Loire. The VUB stable isotope laboratory was upgraded with the support of the Hercules Foundation Flanders.

Appendix A

Table A1
Replicates of NDO2 analyzed at AMMGC stable isotopes laboratory with the Picarro L2130-i

November 2013–February 2017		
N = 121	$\delta^{18}O$ NDO2	δD NDO2
official value	**−7,381**	**−48,80**
5/11/2013	−7,385	−48,90
5/11/2013	−7,340	−48,90
5/11/2013	−7,306	−48,73
14/11/2013	−7,406	−48,93
14/11/2013	−7,363	−48,43
14/11/2013	−7,413	−48,59
27/11/2013	−7,383	−49,39
27/11/2013	−7,345	−48,59
27/11/2013	−7,372	−48,71
3/1/2014	−7,377	−48,93
3/1/2014	−7,345	−48,71
3/1/2014	−7,424	−48,96
16/4/2014	−7,375	−48,91
16/4/2014	−7,386	−48,84
16/4/2014	−7,378	−48,73
16/4/2014	−7,350	−48,61
16/4/2014	−7,382	−49,07
16/4/2014	−7,389	−49,06
16/4/2014	−7,409	−49,03

(*continued on next page*)

Table A1 (*continued*)

November 2013–February 2017		
N = 121	δ^{18}O NDO2	δD NDO2
16/4/2014	−7,386	−48,92
16/4/2014	−7,323	−48,71
16/4/2014	−7,359	−48,75
16/4/2014	−7,385	−48,94
16/4/2014	−7,413	−49,06
16/4/2014	−7,377	−49,03
7/5/2014	−7,388	−48,80
7/5/2014	−7,356	−48,75
7/5/2014	−7,376	−48,82
8/5/2014	−7,329	−48,82
8/5/2014	−7,368	−48,84
8/5/2014	−7,371	−48,88
8/5/2014	−7,377	−48,93
8/5/2014	−7,340	−48,79
8/5/2014	−7,355	−48,73
8/5/2014	−7,347	−48,75
12/5/2014	−7,360	−48,87
12/5/2014	−7,375	−48,88
12/5/2014	−7,343	−48,78
12/5/2014	−7,405	−48,95
2/6/2014	−7,392	−49,04
2/6/2014	−7,421	−48,90
2/6/2014	−7,394	−49,00
2/6/2014	−7,375	−48,92
2/6/2014	−7,410	−49,01
10/6/2014	−7,368	−48,86
10/6/2014	−7,420	−48,99
10/6/2014	-7,363	-48,84
7/3/2014	−7,453	−49,02
3/7/2014	−7,420	−48,87
3/7/2014	−7,367	−48,91
3/7/2014	−7,374	−48,92
9/7/2014	−7,393	−49,02
9/7/2014	−7,396	−48,94
9/7/2014	−7,420	−49,01
9/7/2014	−7,413	−49,17
9/7/2014	−7,413	−49,04
9/7/2014	−7,362	−48,87
11/7/2014	−7,383	−48,92
11/7/2014	−7,378	−48,91
11/7/2014	−7,391	−48,95
12/7/2014	−7,411	−48,96
12/7/2014	−7,391	−49,00
12/7/2014	−7,403	−48,90
12/7/2014	−7,412	−49,00
14/7/2014	−7,423	−49,04
7/14/2014	−7,371	−48,85
14/7/2014	−7,371	−48,91
14/7/2014	−7,408	−48,94
16/7/2014	−7,408	−49,03
16/7/2014	−7,351	−48,79
16/7/2014	−7,385	−48,93
16/7/2014	−7,383	−48,90
19/7/2014	−7,365	−48,91
19/7/2014	−7,381	−48,89
19/7/2014	−7,406	−48,99
19/7/2014	−7,418	−48,98
24/7/2014	−7,399	−48,79
24/7/2014	−7,366	−48,86
24/7/2014	−7,405	−49,11
24/7/2014	−7,407	−48,99
27/7/2014	−7,407	−49,03
27/7/2014	−7,374	−48,79
27/7/2014	−7,366	−48,90
27/7/2014	−7,328	−48,77
29/7/2014	−7,371	−48,82
29/7/2014	−7,408	−49,01

(*continued on next page*)

Table A1 (*continued*)

November 2013–February 2017		
N = 121	δ^{18}O NDO2	δD NDO2
29/7/2014	−7,388	−48,97
29/7/2014	−7,369	−48,77
15/9/2014	−7,366	−49,03
15/9/2014	−7,461	−48,96
14/11/2014	−7,370	−49,06
14/11/2014	−7,322	−48,77
14/11/2014	−7,266	−48,55
15/4/2015	−7,361	−48,64
15/4/2015	−7,404	−48,95
15/4/2015	−7,337	−48,65
15/4/2015	-7,401	-48,84
15/4/2015	−7,473	−48,83
15/4/2015	−7,498	−49,03
4/15/2015	−7,443	−48,94
9/2/2016	−7,345	−48,75
9/2/2016	−7,348	−48,86
9/2/2016	−7,370	−48,93
23/2/2016	−7,353	−48,94
23/2/2016	−7,402	−48,73
23/2/2016	−7,405	−48,81
23/2/2016	−7,370	−48,70
23/2/2016	−7,351	−48,80
23/2/2016	−7,340	−48,95
17/5/2016	−7,358	−48,78
17/5/2016	−7,311	−48,67
17/5/2016	−7,395	−48,64
17/5/2016	−7,409	−48,87
1/6/2016	−7,404	−49,11
1/6/2016	−7,407	−49,00
1/6/2016	−7,368	−48,90
1/6/2016	−7,339	−48,74
1/6/2016	−7,392	−49,08
13/2/2017	−7,384	−48,89
13/2/2017	−7,357	−48,86
13/2/2017	−7,334	−48,73

Appendix B

Table B1
Comparison of domestic water (DW) and waste water (WW) isotope ratios (δ^{18}O and δD) analysed by laser absorption spectroscopy (dry air, N2) with an analytical uncertainty (2σ) of 0,06‰ and 0,4‰, respectively. The analytical uncertainty (2σ) for one measurement of δ^{18}O with the mass spectrometer is 0,1‰. The little differences in δ^{18}O and δD values fall within the analytical uncertainty associated to the measurements made with IRMS and LAS instrument.

Sample code (DW = domestic water, WW = waste water)	δ18O (‰) IRMS	δ18O (‰) dry air	δ18O (‰) N2 gas	δD (‰) dry air	δD (‰) N2 gas
DW 199	−7,11	−7,10	−7,13	−47,3	−47,3
DW 254	−6,92	−6,97	−6,99	−46,8	−47,0
DW 301	−7,12	−7,13	−7,16	−47,7	−47,9
DW 302	−7,22	−7,23	−7,25	−48,2	−48,2
DW 303	−7,31	−7,31	−7,39	−48,6	−49,0
WW B03	−6,96	−6,99	−6,99	−46,6	−46,7
WW B05	−6,97	−6,98	−6,98	−46,7	−46,6
WW B07	−6,90	−6,96	−6,97	−46,6	−46,5
WW B09	−6,90	−6,95	−6,96	−46,5	−46,6
WW B11	−6,93	−6,92	−7,00	−46,4	−46,5
WW B39	−7,11	−7,14	−7,11	−47,9	−47,8
WW B56	−7,10	−7,08	−7,14	−47,5	−47,6
WW B57	−7,12	−7,10	−7,15	−47,5	−47,6
WW B58	−7,16	−7,14	−7,11	−47,9	−47,6

Appendix C

Table C1
Dataset, Isotopic analyses in the article. "SW" refers to stormwater, "WW" to waste water and "GW" to groundwater. The measurements are corrected with in-house standards (NDO1, NDO2 and NDO3) that were previously calibrated in the AMGC laboratory versus the international standards GISP, VSMOW2, SLAP2 (IAEA, 1993). The delta values of the in-house standards are respectively −0.79, −7.38 and −14.77 for $\delta^{18}O$ and −26.2, −48.8 and −105.1 for δD. The analytical uncertainty is evaluated on replicates of NDO2 (minimum 16) for periods of few months. The most recent replicates show an analytical uncertainty of 0,06 and 0,3 for $\delta^{18}O$ and δD respectively (cf. Table A1 in Appendix A).

Brussels

Sampling site	Sampling infrastructure	Sampling day	Water body	$\delta^{18}O$ (‰)	δD (‰)	Analytical uncert. $\delta^{18}O$ (2σ)	Analytical uncert. δD (2σ)
Brussels sector 3	Tap	8/26/2010	Domestic water (Meuse water) sector 3	−6,65	−44,76	0,06	0,3
Brussels sector 3	Tap	9/10/2010	Domestic water (Meuse water) sector 3	−6,61	−44,2	0,06	0,3
Brussels sector 3	Tap	9/22/2010	Domestic water (Meuse water) sector 3	−6,63	−44,9	0,06	0,3
Brussels sector 3	Tap	10/8/2010	Domestic water (Meuse water) sector 3	−6,61	−44,9	0,17	0,9
Brussels sector 3	Tap	10/21/2010	Domestic water (Meuse water) sector 3	−6,81	−45,4	0,17	0,9
Brussels sector 3	Tap	11/8/2010	Domestic water (Meuse water) sector 3	−6,90	−46,0	0,06	0,3
Brussels sector 3	Tap	11/21/2010	Domestic water (Meuse water) sector 3	−6,96	−45,2	0,06	0,3
Brussels sector 3	Tap	12/8/2010	Domestic water (Meuse water) sector 3	−7,27	−48,3	0,06	0,3
Brussels sector 3	Tap	1/5/2011	Domestic water (Meuse water) sector 3	−8,56	−57,6	0,17	0,9
Brussels sector 3	Tap	1/9/2011	Domestic water (Meuse water) sector 3	−7,45	−48,9	0,06	0,3
Brussels sector 3	Tap	1/21/2011	Domestic water (Meuse water) sector 3	−7,85	−52,0	0,06	0,3
Brussels sector 3	Tap	2/4/2011	Domestic water (Meuse water) sector 3	−7,41	−49,3	0,06	0,3
Brussels sector 3	Tap	2/18/2011	Domestic water (Meuse water) sector 3	−7,22	−48,23	0,06	0,3
Brussels sector 3	Tap	3/6/2011	Domestic water (Meuse water) sector 3	−7,36	−49,1	0,06	0,3
Brussels sector 3	Tap	3/20/2011	Domestic water (Meuse water) sector 3	−7,43	−49,4	0,06	0,3
Brussels sector 3	Tap	4/5/2011	Domestic water (Meuse water) sector 3	−7,23	−48,2	0,06	0,3
Brussels sector 3	Tap	1/9/2011	Domestic water (Meuse water) sector 3	−7,45	−48,9	0,06	0,3
Brussels sector 3	Tap	4/17/2011	Domestic water (Meuse water) sector 3	−7,17	−47,7	0,17	0,9
Brussels sector 3	Tap	5/15/2011	Domestic water (Meuse water) sector 3	−6,90	−46,4	0,17	0,9
Brussels sector 3	Tap	5/30/2011	Domestic water (Meuse water) sector 3	−6,60	−44,8	0,17	0,9
Brussels sector 3	Tap	6/12/2011	Domestic water (Meuse water) sector 3	−6,48	−44,3	0,17	0,9
Brussels sector 3	Tap	6/27/2011	Domestic water (Meuse water) sector 3	−6,46	−44,1	0,17	0,9
Brussels sector 3	Tap	7/8/2011	Domestic water (Meuse water) sector 3	−6,30	−42,9	0,17	0,9
Brussels sector 3	Tap	7/15/2011	Domestic water (Meuse water) sector 3	−6,35	−43,4	0,06	0,3
Brussels sector 3	Tap	8/1/2011	Domestic water (Meuse water) sector 3	−6,58	−44,6	0,17	0,9
Brussels sector 3	Tap	8/15/2011	Domestic water (Meuse water) sector 3	−6,69	−45,1	0,17	0,9
Brussels sector 3	Tap	8/23/2011	Domestic water (Meuse water) sector 3	−6,77	−45,7	0,06	0,3
Brussels sector 3	Tap	8/31/2011	Domestic water (Meuse water) sector 3	−6,35	−43,1	0,06	0,3
Brussels sector 3	Tap	9/20/2011	Domestic water (Meuse water) sector 3	−6,19	−42,4	0,06	0,3
Brussels sector 3	Tap	10/9/2011	Domestic water (Meuse water) sector 3	−6,93	−46,0	0,06	0,3
Brussels sector 3	Tap	10/28/2011	Domestic water (Meuse water) sector 3	−6,61	−44,4	0,06	0,3
Brussels sector 3	Tap	11/22/2011	Domestic water (Meuse water) sector 3	−6,84	−45,8	0,06	0,3
Brussels sector 3	Tap	12/9/2011	Domestic water (Meuse water) sector 3	−7,03	−46,7	0,17	0,9
Brussels sector 3	Tap	12/19/2011	Domestic water (Meuse water) sector 3	−7,23	−47,5	0,06	0,3
Brussels sector 3	Tap	1/3/2012	Domestic water (Meuse water) sector 3	−7,53	−50,1	0,06	0,3
Brussels sector 3	Tap	1/11/2012	Domestic water (Meuse water) sector 3	−7,37	−47,6	0,06	0,3
Brussels sector 3	Tap	1/23/2012	Domestic water (Meuse water) sector 3	−7,34	−48,2	0,06	0,3
Brussels sector 3	Tap	1/29/2012	Domestic water (Meuse water) sector 3	−7,37	−48,1	0,06	0,3

(*continued on next page*)

Table C1 (*continued*)

Brussels							
Sampling site	Sampling infrastructure	Sampling day	Water body	$\delta^{18}O$ (‰)	δD (‰)	Analytical uncert. $\delta^{18}O$ (2σ)	Analytical uncert. δD (2σ)
Brussels sector 3	Tap	2/1/2012	Domestic water (Meuse water) sector 3	−7,33	−47,4	0,06	0,3
Brussels sector 3	Tap	2/6/2012	Domestic water (Meuse water) sector 3	−7,36	−48,3	0,06	0,3
Brussels sector 3	Tap	2/20/2012	Domestic water (Meuse water) sector 3	−7,27	−48,0	0,06	0,3
Brussels sector 3	Tap	3/5/2012	Domestic water (Meuse water) sector 3	−7,41	−48,7	0,06	0,3
Brussels sector 3	Tap	3/20/2012	Domestic water (Meuse water) sector 3	−7,37	−48,8	0,06	0,3
Brussels sector 3	Tap	4/2/2012	Domestic water (Meuse water) sector 3	−7,30	−48,0	0,06	0,3
Brussels sector 3	Tap	4/16/2012	Domestic water (Meuse water) sector 3	−7,35	−48,4	0,06	0,3
Brussels sector 3	Tap	4/30/2012	Domestic water (Meuse water) sector 3	−7,34	−48,3	0,06	0,3
Brussels sector 3	Tap	5/14/2012	Domestic water (Meuse water) sector 3	−7,25	−48,1	0,06	0,3
Brussels sector 3	Tap	6/11/2012	Domestic water (Meuse water) sector 3	−7,15	−47,2	0,06	0,3
Brussels sector 3	Tap	6/25/2012	Domestic water (Meuse water) sector 3	−7,14	−47,5	0,06	0,3
Brussels sector 3	Tap	7/23/2012	Domestic water (Meuse water) sector 3	−7,27	−48,1	0,06	0,3
Brussels sector 3	Tap	8/6/2012	Domestic water (Meuse water) sector 3	−7,01	−45,7	0,06	0,3
Brussels sector 3	Tap	8/20/2012	Domestic water (Meuse water) sector 3	−6,94	−45,9	0,06	0,3
Brussels sector 3	Tap	9/3/2012	Domestic water (Meuse water) sector 3	−7,01	−46,9	0,09	0,6
Brussels sector 3	Tap	9/17/2012	Domestic water (Meuse water) sector 3	−6,68	−45,4	0,06	0,3
Brussels sector 3	Tap	10/1/2012	Domestic water (Meuse water) sector 3	−6,97	−46,5	0,06	0,3
Brussels sector 3	Tap	10/15/2012	Domestic water (Meuse water) sector 3	−7,16	−47,7	0,06	0,3
Brussels sector 3	Tap	10/30/2012	Domestic water (Meuse water) sector 3	−7,26	−48,0	0,06	0,3
Brussels sector 2	Tap	9/4/2012	Domestic water (mix GW + Meuse) sector 2	−7,13	−47,3	0,09	0,6
Brussels sector 2	Tap	9/4/2012	Domestic water (mix GW + Meuse) sector 2	−6,99	−47,0	0,09	0,6
Brussels sector 1	Tap	9/4/2012	Domestic water (mix of different GW) sector 1	−6,95	−46,5	0,09	0,6
Brussels sector 1	Tap	7/8/2013	Domestic water (mix of different GW) sector 1	−7,16	−47,9	0,09	0,6
Brussels sector 1	Tap	7/8/2013	Domestic water (mix of different GW) sector 1	−7,25	−48,2	0,09	0,6
Brussels sector 1	Tap	7/8/2013	Domestic water (mix of different GW) sector 1	−7,39	−49,0	0,09	0,6
Brussels sector 1	Tap	9/10/2014	Domestic water (mix of different GW) sector 1	−7,25	−47,3	0,06	0,3
Brussels sector 1	Tap	9/10/2014	Domestic water (mix of different GW) sector 1	−7,20	−47,1	0,06	0,3
Brussels sector 1	Tap	9/10/2014	Domestic water (mix of different GW) sector 1	−7,28	−47,4	0,06	0,3
312	pumping station	6/21/2011	"Ypresian Hills" aquifer system	−7,18	−47,3	0,17	0,9
312	pumping station	6/20/2012	"Ypresian Hills" aquifer system	−7,14	−47,3	0,09	0,6
312	pumping station	12/14/2012	"Ypresian Hills" aquifer system	−7,17	−47,3	0,12	0,8
P34	pumping station	12/14/2012	"Ypresian Hills" aquifer system	−7,20	−46,9	0,12	0,8
Eikelenberg	spring	1/11/2012	"Ypresian Hills" aquifer system	−7,16	−47,0	0,17	0,9
Eikelenberg	spring	2/1/2012	"Ypresian Hills" aquifer system	−7,00	−46,5	0,17	0,9
Eikelenberg	spring	11/29/2010	"Ypresian Hills" aquifer system	−6,99	−45,5	0,17	0,9
Mol P1	spring	2/4/2011	"Ypresian Hills" aquifer system	−7,14	−46,8	0,17	0,9
Mol P1	spring	5/2/2011	"Ypresian Hills" aquifer system	−7,10	−46,8	0,17	0,9
Mol P1	spring	5/30/2011	"Ypresian Hills" aquifer system	−7,18	−47,1	0,17	0,9
Mol P1	spring	6/27/2011	"Ypresian Hills" aquifer system	−7,20	−47,1	0,17	0,9
Mol P1	spring	8/1/2011	"Ypresian Hills" aquifer system	−7,08	−46,8	0,17	0,9
Mol P1	spring	8/31/2011	"Ypresian Hills" aquifer system	−7,05	−46,4	0,17	0,9
Mol P1	spring	9/26/2011	"Ypresian Hills" aquifer system	−7,06	−46,7	0,17	0,9
Mol P1	spring	10/17/2011	"Ypresian Hills" aquifer system	−7,12	−46,9	0,17	0,9
Mol P1	spring	11/22/2011	"Ypresian Hills" aquifer system	−7,14	−46,9	0,17	0,9
Mol P1	spring	1/11/2012	"Ypresian Hills" aquifer system	−7,04	−46,9	0,17	0,9
Mol P4	spring	1/5/2011	"Ypresian Hills" aquifer system	−7,22	−47,7	0,17	0,9
Mol P4	spring	5/30/2011	"Ypresian Hills" aquifer system	−7,05	−46,7	0,17	0,9

(*continued on next page*)

Table C1 (*continued*)

Brussels							
Sampling site	Sampling infrastructure	Sampling day	Water body	$\delta^{18}O$ (‰)	δD (‰)	Analytical uncert. $\delta^{18}O$ (2σ)	Analytical uncert. δD (2σ)
Mol P4	spring	6/27/2011	"Ypresian Hills" aquifer system	−6,99	−46,0	0,17	0,9
Mol P4	spring	8/1/2011	"Ypresian Hills" aquifer system	−6,94	−44,9	0,17	0,9
Mol P4	spring	8/31/2011	"Ypresian Hills" aquifer system	−6,46	−42,1	0,17	0,9
Mol P4	spring	9/26/2011	"Ypresian Hills" aquifer system	−6,92	−46,0	0,17	0,9
Mol P4	spring	10/17/2011	"Ypresian Hills" aquifer system	−6,96	−45,9	0,17	0,9
Mol P4	spring	11/22/2011	"Ypresian Hills" aquifer system	−7,04	−46,4	0,17	0,9
Mol P4	spring	1/11/2012	"Ypresian Hills" aquifer system	−7,05	−46,5	0,17	0,9
Thaborberg	spring	4/5/2011	"Ypresian Hills" aquifer system	−6,48	−42,9	0,17	0,9
Thaborberg	spring	5/2/2011	"Ypresian Hills" aquifer system	−6,46	−43,2	0,17	0,9
Thaborberg	spring	5/30/2011	"Ypresian Hills" aquifer system	−6,44	−42,7	0,17	0,9
Thaborberg	spring	6/27/2011	"Ypresian Hills" aquifer system	−6,53	−42,8	0,17	0,9
Thaborberg	spring	8/1/2011	"Ypresian Hills" aquifer system	−7,01	−46.4	0,17	0,9
Thaborberg	spring	8/31/2011	"Ypresian Hills" aquifer system	−6,70	−44,5	0,17	0,9
Thaborberg	spring	9/26/2011	"Ypresian Hills" aquifer system	−6,50	−43,0	0,17	0,9
Thaborberg	spring	10/17/2011	"Ypresian Hills" aquifer system	−6,58	−42,9	0,17	0,9
Thaborberg	spring	11/22/2011	"Ypresian Hills" aquifer system	−6,93	−45,3	0,17	0,9
Thaborberg	spring	1/11/2012	"Ypresian Hills" aquifer system	−6,82	−44,5	0,17	0,9
RB P1	spring	11/29/2010	"Ypresian Hills" aquifer system	−7,24	−47,2	0,17	0,9
RB P1	spring	8/31/2011	"Ypresian Hills" aquifer system	−6,52	−43,7	0,17	0,9
RB P1	spring	1/11/2012	"Ypresian Hills" aquifer system	−7,16	−46,8	0,17	0,9
RB P2	spring	2/4/2011	"Ypresian Hills" aquifer system	−7,03	−46,0	0,17	0,9
RB P2	spring	5/2/2011	"Ypresian Hills" aquifer system	−6,86	−44,8	0,17	0,9
RB P2	spring	5/30/2011	"Ypresian Hills" aquifer system	−7,02	−45,6	0,17	0,9
RB P2	spring	6/27/2011	"Ypresian Hills" aquifer system	−6,94	−45,2	0,17	0,9
RB P3	spring	8/1/2011	"Ypresian Hills" aquifer system	−7,04	−45,7	0,17	0,9
RB P3	spring	9/26/2011	"Ypresian Hills" aquifer system	−6,91	−45,3	0,17	0,9
RB P3	spring	11/22/2011	"Ypresian Hills" aquifer system	−6,99	−45,7	0,17	0,9
RB P3	spring	1/11/2012	"Ypresian Hills" aquifer system	−7,10	−46,5	0,17	0,9
315	pumping station	9/22/2011	Brussels sands aquifer system	−7,28	−48,4	0,17	0,9
315	pumping station	5/23/2012	Brussels sands aquifer system	−7,11	−48,1	0,06	0,4
315	pumping station	9/19/2012	Brussels sands aquifer system	−7,24	−48,5	0,06	0,4
P11	pumping station	9/20/2011	Brussels sands aquifer system	−7,30	−48,5	0,17	0,9
P11	pumping station	5/23/2012	Brussels sands aquifer system	−7,28	−48,4	0,06	0,4
P11	pumping station	9/20/2012	Brussels sands aquifer system	−7,29	−48,4	0,06	0,4
P12	pumping station	9/21/2011	Brussels sands aquifer system	−7,04	−47,2	0,17	0,9
P12	pumping station	5/22/2012	Brussels sands aquifer system	−6,89	−46,9	0,06	0,4
P12	pumping station	9/19/2012	Brussels sands aquifer system	−7,00	−47,1	0,06	0,4
P13	pumping station	9/20/2011	Brussels sands aquifer system	−7,11	−47,4	0,17	0,9
P13	pumping station	5/22/2012	Brussels sands aquifer system	−7,07	−47,4	0,06	0,4
P13	pumping station	9/18/2012	Brussels sands aquifer system	−7,05	−47,4	0,06	0,4
P14	pumping station	9/21/2011	Brussels sands aquifer system	−7,16	−47,6	0,17	0,9
P14	pumping station	5/24/2012	Brussels sands aquifer system	−7,04	−47,3	0,06	0,4
P14	pumping station	9/20/2012	Brussels sands aquifer system	−7,12	−47,7	0,06	0,4
P28	pumping station	5/28/2012	Brussels sands aquifer system	−7,21	−47,9	0,06	0,4
P28	pumping station	9/28/2012	Brussels sands aquifer system	−7,22	−48,0	0,06	0,4
P29	pumping station	9/22/2011	Brussels sands aquifer system	−7,33	−48,5	0,17	0,9
P29	pumping station	5/30/2012	Brussels sands aquifer system	−7,33	−48,7	0,09	0,6

(*continued on next page*)

Table C1 (*continued*)

Brussels							
Sampling site	Sampling infrastructure	Sampling day	Water body	$\delta^{18}O$ (‰)	δD (‰)	Analytical uncert. $\delta^{18}O$ (2σ)	Analytical uncert. δD (2σ)
P29	pumping station	9/28/2012	Brussels sands aquifer system	−7,32	−48,7	0,06	0,4
P31	pumping station	9/20/2011	Brussels sands aquifer system	−7,14	−47,8	0,17	0,9
P31	pumping station	5/22/2012	Brussels sands aquifer system	−7,11	−48,0	0,06	0,4
P31	pumping station	9/18/2012	Brussels sands aquifer system	−7,14	−47,9	0,06	0,4
P6	pumping station	9/20/2011	Brussels sands aquifer system	−7,29	−48,4	0,17	0,9
P6	pumping station	7/3/2012	Brussels sands aquifer system	−7,35	−48,5	0,12	0,8
P6	pumping station	12/4/2012	Brussels sands aquifer system	−7,33	−48,5	0,12	0,8
P8	pumping station	9/20/2011	Brussels sands aquifer system	−7,20	−48,1	0,17	0,9
P8	pumping station	7/3/2012	Brussels sands aquifer system	−7.18	−48.3	0.12	0.8
P8	pumping station	12/10/2012	Brussels sands aquifer system	−7,20	−48,3	0,12	0,8
ST32	pumping station	9/23/2011	Brussels sands aquifer system	−7,14	−47,6	0,17	0,9
ST32	pumping station	6/21/2012	Brussels sands aquifer system	−7,11	−47,4	0,12	0,8
ST32	pumping station	12/7/2012	Brussels sands aquifer system	−7,16	−47,6	0,12	0,8
WW003	combined sewer	9/4/2012	Sewer water − Sector 2	−6,99	−46,7	0,09	0,6
WW005	combined sewer	9/4/2012	Sewer water − Sector 2	−6,98	−46,6	0,09	0,6
WW007	combined sewer	9/4/2012	Sewer water − Sector 2	−6,97	−46,5	0,09	0,6
WW009	combined sewer	9/4/2012	Sewer water − Sector 2	−6,96	−46,6	0,09	0,6
WW011	combined sewer	9/4/2012	Sewer water − Sector 2	−7,00	−46,5	0,,09	0,6
WW021	combined sewer	9/4/2012	Sewer water − Sector 1	−6,87	−46,1	0,09	0,6
WW023	combined sewer	9/4/2012	Sewer water − Sector 1	−6,86	−45,9	0,09	0,6
WW025	combined sewer	9/4/2012	Sewer water − Sector 1	−6,90	−46,1	0,09	0,6
WW027	combined sewer	9/4/2012	Sewer water − Sector 1	−6,82	−46,0	0,09	0,6
WW029	combined sewer	9/4/2012	Sewer water − Sector 1	−6,88	−46,2	0,09	0,6
WW031	combined sewer	9/4/2012	Sewer water − Sector 1	−6,89	−46,3	0,09	0,6
WW033	combined sewer	9/4/2012	Sewer water − Sector 1	−6,83	−46,2	0,09	0,6
WW039	combined sewer	7/8/2013	Sewer water − Sector 1	−7,11	−47,8	0,09	0,6
WW056	combined sewer	7/8/2013	Sewer water − Sector 1	−7,14	−47,6	0,09	0,6
WW057	combined sewer	7/8/2013	Sewer water − Sector 1	−7,15	−47,6	0,09	0,6
WW058	combined sewer	7/8/2013	Sewer water − Sector 1	−7,11	−47,6	0,09	0,6
WW065	combined sewer	9/10/2014	Sewer water − Sector 1	−6,99	−46,1	0,06	0,3
WW066	combined sewer	9/10/2014	Sewer water − Sector 1	−7,05	−46,2	0,06	0,3
WW067	combined sewer	9/10/2014	Sewer water − Sector 1	−7,08	−46,3	0,06	0,3
WW068	combined sewer	9/10/2014	Sewer water − Sector 1	−7,03	−46,0	0,06	0,3
WW069	combined sewer	9/10/2014	Sewer water − Sector 1	−7,12	−46,4	0,06	0,3
WW070	combined sewer	9/10/2014	Sewer water − Sector 1	−7,07	−46,1	0,06	0,3
WW071	combined sewer	9/10/2014	Sewer water − Sector 1	−7,11	−46,4	0,06	0,3
WW072	combined sewer	9/10/2014	Sewer water − Sector 1	−7,14	−46,5	0,06	0,3
WW073	combined sewer	9/10/2014	Sewer water − Sector 1	−7,13	−46,5	0,06	0,3
WW074	combined sewer	9/10/2014	Sewer water − Sector 1	−7,25	−47,2	0,06	0,3
WW075	combined sewer	9/10/2014	Sewer water − Sector 1	−6,60	−45,2	0,06	0,3
WW076	combined sewer	9/10/2014	Sewer water − Sector 1	−7.04	−46.5	0,06	0,3

(*continued on next page*)

Table C1 (*continued*)

Nantes							
Sampling site name	Sampling infrastructure	Sampling day	Water body	$\delta^{18}O$ (‰)	δD (‰)	$\delta^{18}O$ uncertain (2σ)	δD uncertain (2σ)
Nantes	tap	10/2/2012	domestic water (Loire water)	−5,23	−37,7	0,06	0,4
Nantes	tap	11/5/2012	domestic water (Loire water)	−5,63	−38,8	0,06	0,4
Nantes	tap	12/3/2012	domestic water (Loire water)	−5,77	−39,0	0,06	0,4
Nantes	tap	1/4/2013	domestic water (Loire water)	−5,87	−39,1	0,06	0,4
Nantes	tap	2/1/2013	domestic water (Loire water)	−6,12	−40,6	0,06	0,4
Nantes	tap	3/6/2013	domestic water (Loire water)	−6,28	−41,6	0,06	0,4
Nantes	tap	4/3/2013	domestic water (Loire water)	−6,45	−42,8	0,06	0,4
Nantes	tap	5/16/2013	domestic water (Loire water)	−7,16	−47,8	0,09	0,6
Nantes	tap	6/3/2013	domestic water (Loire water)	−6,25	−43,0	0,06	0,4
Nantes	tap	6/28/2013	domestic water (Loire water)	−6,52	−44,4	0,06	0,4
Nantes	tap	8/2/2013	domestic water (Loire water)	−6,42	−43,3	0,06	0,4
Nantes	tap	9/13/2013	domestic water (Loire water)	−6,07	−41,6	0,06	0,4
Nantes	tap	10/3/2013	domestic water (Loire water)	−6,10	−41,5	0,06	0,4
Nantes	tap	11/4/2013	domestic water (Loire water)	−6,13	−41,6	0,06	0,4
Nantes	tap	12/2/2013	domestic water (Loire water)	−5,53	−39,9	0,06	0,4
Nantes	tap	1/7/2014	domestic water (Loire water)	−4,41	−36,8	0,06	0,4
Nantes	tap	2/11/2014	domestic water (Loire water)	−6,58	−43,7	0,06	0,4
Nantes	tap	3/3/2014	domestic water (Loire water)	−6,69	−44,4	0,05	0,4
Nantes	tap	3/12/2014	domestic water (Loire water)	−7,08	−46,6	0,05	0,4
Nantes	tap	4/30/2014	domestic water (Loire water)	−6,71	−44,6	0,05	0,4
Nantes	tap	6/2/2014	domestic water (Loire water)	−6,38	−43,0	0,05	0,4
Nantes	tap	6/16/2014	domestic water (Loire water)	−5,91	−40,2	0,05	0,4
PZBA	piezometer	2/20/2013	groundwater Chézine	−5,28	−32,4	0,10	0,6
PZBA	piezometer	6/26/2013	groundwater Chézine	−5,26	−32,2	0,06	0,4
PZEF	piezometer	2/20/2013	groundwater Chézine	−5,52	−32,5	0,10	0,6
PZEF	piezometer	6/26/2013	groundwater Chézine	−5,46	−32,2	0,06	0,4
PZPJ	piezometer	2/20/2013	groundwater Chézine	−5,44	−32,5	0,10	0,6
PZPJ	piezometer	6/26/2013	groundwater Chézine	−5,54	−33,0	0,06	0,4
PZAF	piezometer	4/3/2013	groundwater Pin-Sec	−5,54	−35,0	0,06	0,4
PZAF	piezometer	5/23/2013	groundwater Pin-Sec	−5,53	−35,2	0,09	0,6
PZAF	piezometer	8/2/2013	groundwater Pin-Sec	−5,51	−34,9	0,06	0,4
PZAF	piezometer	3/12/2014	groundwater Pin-Sec	−5,53	−35,2	0,05	0,4
PZAF	piezometer	6/16/2014	groundwater Pin-Sec	−5,51	−35,2	0,05	0,4
PZCPS	piezometer	2/20/2013	groundwater Pin-Sec	−5,47	−33,0	0,06	0,4
PZCPS	piezometer	4/3/2013	groundwater Pin-Sec	−5,45	−33,0	0,06	0,4
PZCPS	piezometer	5/23/2013	groundwater Pin-Sec	−5,42	−32,9	0,09	0,6
PZCPS	piezometer	8/2/2013	groundwater Pin-Sec	−5,55	−35,8	0,06	0,4
PZCPS	piezometer	3/12/2014	groundwater Pin-Sec	−5,43	−33,1	0,05	0,4
PZCPS	piezometer	6/16/2014	groundwater Pin-Sec	−5,32	−32,6	0,05	0,4
PZCS	piezometer	4/3/2013	groundwater Pin-Sec	−5,33	−33,2	0,06	0,4
PZCS	piezometer	5/23/2013	groundwater Pin-Sec	−5,32	−33,5	0,09	0,6
PZCS	piezometer	8/2/2013	groundwater Pin-Sec	−5,31	−33,5	0,06	0,4
PZCS	piezometer	3/12/2014	groundwater Pin-Sec	−5,34	−33,8	0,05	0,4
PZCS	piezometer	6/16/2014	groundwater Pin-Sec	−5,35	−33,5	0,05	0,4
PZD	piezometer	2/20/2013	groundwater Pin-Sec	−5,34	−33,3	0,06	0,4
PZD	piezometer	4/3/2013	groundwater Pin-Sec	−5,32	−33,5	0,06	0,4
PZD	piezometer	5/23/2013	groundwater Pin-Sec	−5,35	−33,9	0,09	0,6

(*continued on next page*)

Table C1 (*continued*)

Nantes							
Sampling site name	Sampling infrastructure	Sampling day	Water body	$\delta^{18}O$ (‰)	δD (‰)	$\delta^{18}O$ uncertain (2σ)	δD uncertain (2σ)
PZD	piezometer	8/2/2013	groundwater Pin-Sec	−5,34	−33,9	0,06	0,4
PZD	piezometer	3/12/2014	groundwater Pin-Sec	−5,30	−33,9	0,05	0,4
PZD	piezometer	6/16/2014	groundwater Pin-Sec	−5,34	−34,3	0,05	0,4
PZPS	piezometer	4/3/2013	groundwater Pin-Sec	−5,58	−35,5	0,06	0,4
PZPS	piezometer	5/23/2013	groundwater Pin-Sec	−5,57	−35,7	0,09	0,6
PZPS	piezometer	3/12/2014	groundwater Pin-Sec	−5,57	−35,6	0,05	0,4
PZPS	piezometer	6/16/2014	groundwater Pin-Sec	−5,51	−35,4	0,05	0,4
1 a	SW sewer	5/16/2013	sewer water Pin-sec	−5,38	−35,28	0,09	0,6
1 b	SW sewer	5/16/2013	sewer water Pin-sec	−5,29	−33,22	0,09	0,6
2	SW sewer	5/16/2013	sewer water Pin-sec	−5,40	−33,90	0,09	0,6
3	SW sewer	5/16/2013	sewer water Pin-sec	−5,48	−34,44	0,09	0,6
4	SW sewer	5/16/2013	sewer water Pin-sec	−5,38	−34,17	0,09	0,6
5	SW sewer	5/16/2013	sewer water Pin-sec	−5,43	−34,18	0,09	0,6
6	SW sewer	5/16/2013	sewer water Pin-sec	−5,40	−34,09	0,09	0,6
7	WW sewer	5/16/2013	sewer water Pin-sec	−6,15	−39,72	0,09	0,6
8	WW sewer	5/16/2013	sewer water Pin-sec	−6,76	−44.07	0,09	0,6
9	WW sewer	5/16/2013	sewer water Pin-sec	−6.21	−39,89	0,09	0,6
10	WW sewer	5/16/2013	sewer water Pin-sec	−6.46	−43,13	0,09	0,6
11	WW sewer	5/16/2013	sewer water Pin-sec	−6,77	−44,57	0,09	0,6
12	WW sewer	5/16/2013	sewer water Pin-sec	−6,84	−45,18	0,09	0,6
13	WW sewer	5/16/2013	sewer water Pin-sec	−6,81	−46,25	0,09	0,6
14	WW sewer	5/16/2013	sewer water Pin-sec	−6,94	−46,07	0,09	0,6
15	WW sewer	5/16/2013	sewer water Pin-sec	−6,91	−45.67	0,09	0.6
1	SW sewer	3/12/2014	sewer water Pin-sec	−5,35	−32.40	0,05	0,4
2	SW sewer	3/12/2014	sewer water Pin-sec	−5,42	−32,98	0,05	0,4
3	SW sewer	3/12/2014	sewer water Pin-sec	−5,49	−33,12	0,05	0,4
4	SW sewer	3/12/2014	sewer water Pin-sec	−5.45	−33,40	0,05	0,4
5	SW sewer	3/12/2014	sewer water Pin-sec	−5,90	−36,74	0,05	0,4
6	SW sewer	3/12/2014	sewer water Pin-sec	−6,12	−38,18	0,05	0,4
7	WW sewer	3/12/2014	sewer water Pin-sec	−6,37	−40,60	0,05	0,4
8	WW sewer	3/12/2014	sewer water Pin-sec	−6,67	−42,87	0,05	0,4
9	WW sewer	3/12/2014	sewer water Pin-sec	−6,69	−43,23	0,05	0,4
10	WW sewer	3/12/2014	sewer water Pin-sec	−6,82	−44,25	0,05	0,4
11	WW sewer	3/12/2014	sewer water Pin-sec	−6.83	−44,44	0,05	0,4
12	WW sewer	3/12/2014	sewer water Pin-sec	−6.87	−44,56	0,05	0,4
13	WW sewer	3/12/2014	sewer water Pin-sec	−6,86	−44,56	0,05	0,4
14	WW sewer	3/12/2014	sewer water Pin-sec	−6,91	−44,92	0,05	0,4
15	WW sewer	3/12/2014	sewer water Pin-sec	−7,01	−45,44	0,05	0,4

Appendix D

Table D1
Isotopic composition of rain events in Nantes.

Nantes							
Sampling site name	Sampling infrastructure	Sampling day	Water body	$\delta^{18}O$ (‰)	δD (‰)	$\delta^{18}O$ uncert. (2σ)	δD uncert. (2σ)
Chézine	rain gauge	12/20/2012	rainwater	−5,88	−37,2	0,06	0,4
Chézine	rain gauge	1/14/2013	rainwater	−6,74	−36,8	0,06	0,4
Chézine	rain gauge	2/5/2013	rainwater	−7,46	−56,0	0,06	0,4
Chézine	rain gauge	4/9/2013	rainwater	−9,83	−66,5	0,06	0,4
Chézine	rain gauge	4/11/2013	rainwater	−4,78	−26,5	0,06	0,4
Chézine	rain gauge	6/3/2013	rainwater	−7,76	−54,0	0,06	0,4
Chézine	rain gauge	6/14/2013	rainwater	−4,93	−37,8	0,06	0,4
Chézine	rain gauge	6/28/2013	rainwater	−2,84	−17,9	0,06	0,4
Chézine	rain gauge	7/9/2013	rainwater	−6,13	−34,3	0,06	0,4
Chézine	rain gauge	8/2/2013	rainwater	−5,50	−35,4	0,06	0,4
Chézine	rain gauge	9/4/2013	rainwater	−1,82	−6,1	0,06	0,4
Chézine	rain gauge	9/17/2013	rainwater	−6,97	−46,0	0,06	0,4
Chézine	rain gauge	10/10/2013	rainwater	−5,04	−28,5	0,06	0,4
Chézine	rain gauge	10/18/2013	rainwater	−6,35	−36,6	0,06	0,4
Chézine	rain gauge	11/2/2013	rainwater	−0,94	−0,9	0,06	0,4
Chézine	rain gauge	11/18/2013	rainwater	−6,07	−32,3	0,06	0,4
Chézine	rain gauge	12/19/2013	rainwater	−5,53	−26,6	0,06	0,4
Pin-Sec	rain gauge	7/29/2013	rainwater	−3,45	−22,6	0,06	0,4
Pin-Sec	rain gauge	10/3/2013	rainwater	−5,92	−39,1	0,06	0,4
Pin-Sec	rain gauge	10/16/2013	rainwater	−6,92	−45,7	0,06	0,4
Pin-Sec	rain gauge	6/4/2014	rainwater	−4,33	−26,3	0,06	0,4

References

Almeida, M.C., Butler, D., Friedler, E., 1999. At-source domestic wastewater quality. Urban Water 1, 49–55.

Astee, 2015. Patrimonial Management of Sewer Systems: Good Practices + Technical and Financing Aspects (in French). Guide. 248p. (https://www.astee.org/site/wp-content/uploads/2016/02/ASTEE-Guide_GPRA_VF.pdf, Accessed January 2018).

Barth, J.A.C., Veizer, J., 2004. Water mixing in a St. Lawrence river embayment to outline potential sources of pollution. Appl. Geochem. 19 (41), 1637–1641.

Barthold, F., Tyralla, C., Schneider, K., Vache, K., Frede, H.-G., Breuer, L., 2011. How many tracers do we need for end member mixing analysis (EMMA)? A sensitivity analysis. Water Resour. Res. 47, W08519.

Belhadj, N., Joannis, C., Raimbault, G., 1995. Modelling of rainfall induced infiltration into separate sewerage. Water Sci. Technol. 32 (1), 161–168.

Berman, E.S., Gupta, M., Gabrielli, C., Garland, T., McDonnell, J.J., 2009. High-frequency field-deployable isotope analyzer for hydrological applications. Water Resour. Res. 45, 1–7.

Bertrand-Krajewski, J.L., Laplace, D., Joannis, C., Chebbo, G., 2000. Mesures en hydrologie urbaine et assainissement. Lavoisier Tec et Doc, Paris, France (794 p. ISBN 2-7430-0380-4).

Broadhead, A.T., Horn, R., Lerner, D.N., 2013. Captured streams and springs in combined sewers: a review of the evidence, consequences and opportunities. Water Res. 47, 4752–4766.

Brussels Environment, 2011. In: Hannequart, J.-P., Schamp, E. (Eds.), Environmental Impact of the Water Management Planning of the Brussels-Capital Region. Public report in French. 352 p. (Accessed June 2016: http://www.environnement.brussels/doc).

Buffel, P., Matthijs, J., 2008. Explicative Report on the Geological Map of Belgium 31–39 Brussels-Nijvel (in Dutch), report of the Belgium Geological Service. (49p).

Burns, D., McDonnell, J., Hooper, R., Peters, N., Freer, J., Kendall, C., Beven, K., 2001. Quantifying contributions to storm runoff through end-member mixing analysis and hydrologic measurements at panola mountain Research Watershed (Georgia, USA). Hydrol. Processes 15, 1903–1924.

Christophersen, N., Neal, C., Hooper, R., Vogt, R., Andersen, S., 1990. Modelling streamwater chemistry as a mixture of soilwater end-members: a step towards second-generation acidifciation models. J. Hydrol. 116, 307–320.

Dam, J.P., Nuyens, J., Roisin, V., Thonnard, R., 1986. Geotechnical map of Brussel 31-7-3. Ministery of Public Works.

De Bénédittis, J., Bertrand-Krajewski, J.L., 2005a. Infiltration in sewer systems: comparison of measurement methods. Water Sci. Technol. 52, 219–227.

De Bénédittis, J., Bertrand-Krajewski, J.L., 2005b. Measurement of infiltration rates in urban sewer systems by use of oxygen isotopess. Water Sci. Technol. 52, 229–237.

De Bondt, K., Claeys, Ph., 2015. Stable isotopes ((^{18}O and (D) analyses to identify the main sources of aquifer recharge in the Brussels Capital Region (Belgium). In: Brebbia, C. (Ed.), WIT Transaction on Ecology and the Environment ? Water Resource Management VIII. WIT Press, 183-193 (SBN: 978-1-84564-960-9).

Dirckx, G., Bixio, D., Thoeye, C., De Gueldre, G., Van De Steene, B., 2009. Dilution of sewage in Flanders mapped with mathematical and tracer methods. Urban Waters J. 6 (2), 81–92.

Ellis, T.B., Butler, D., 2015. Surface water sewer misconnections in England and wales: pollution sources and impacts. Sci. Total Environ. 526, 98–109.

European Environment Agency, 2015. The Biogeographical Regions of Europe. (data Accessed June 2016: http://www.eea.europa.eu/data-and-maps/data/biogeographical-regions-europe).

Houhou, J., Lartiges, B.S., France-Lanord, C., Guilmette, C., Poix, S., Mustin, C., 2010. Isotopic tracing of clear water sources in an urban sewer: a combined water and dissolved sulfate stable isotope approach. Water Res. 44, 256–266.

IAEA, USGS, 2013. A laboratory information management system for stable hydrogen and oxygen isotopes in water samples by laser absorption spectroscopy. User Manual Tutorial, v1.5 (160p.).

IAEA, 2000a. Environmental isotopes in the hydrological cycle: principles and applications. In: In: Mook, W. (Ed.), Introduction, Theory, Methods, Review, vol. 1. IAEA & UNESCO publications, Vienna, pp. 1–164.

IAEA, 2000b. In: Rozanski, K., Froelich, K., Mook, W. (Eds.), Environmental Isotopes in the Hydrological Cycle: Principles and Applications, Volume 3, Surface Water. IAEA & UNESCO publications, Vienna, pp. 239–311.

IAEA, 2002. The Application of Isotope Techniques to the Assessment of Aquifer Systems in Major Urban Areas. IAEA publication technical document 1298 (179p).

Irvine, K., Rossi, M.C., Vermette, S., Bakert, J., Kleinfelder, K., 2011. Illicit discharge detection and elimination: low cost options for source identification and trackdown in stormwater systems. Urban Water J. 8 (6), 379–395.
JCGM, 2008. Evaluation of measurement data: guide to the expression of uncertainty in measurement. JCGM/WC 1 Report (120 p.).
JCGM, 2012. International vocabulary of metrology –Basic and general concepts and associated terms (VIM), 3rd edition. JCGM Report (92 p.).
Joannis, C., Hannouche, A., Chebbo, G., 2015. An assessment of the respective contributions of flow-rate and concentration variations to mass discharge variations at the outlets of two combined catchments during rain events. Urban Water J. 12 (8), 653–659.
Kim, J., Soo Lim, J., Friedman, J., Lee, U., Vieira, L., Rosso, D., Gerla, M., Srivastava, M.B., 2009. Sensor, mesh and ad hoc. 6th Annual IEEE Communications Society Conference on Communications and Networks, 22–26 June (9p.).
Klaus, J., McDonnell, J., 2013. Hydrograph separation using stable isotopes: review and evaluation. J. Hydrol. 505, 47–64.
Klaus, J., Chun, K., McGuire, K., McDonnell, J., 2015. Temporal dynamics of catchment transit times from stable isotope data. Water Resour. Res. 51, 4208–4223.
Kracht, O., Gujer, W., 2005. Quantification of infiltration into sewers based on time series of pollutant loads. Water Sci. Technol. 52 (3), 209–218.
Kracht, O., Gresch, M., Gujer, W., 2007. A stable isotope approach for the quantification of sewer infiltration. Environ. Sci. Technol. 41, 5839–5845.
Le Delliou, A.-L., Rodiguez, F., Andrieu, H., 2009. Hydrological modelling of sewer network impacts on urban groundwater (in French). La Houille Blanche 5, 152–158.
Liu, F., Parmenter, R., Brooks, P., Conklin, M., Bales, R., 2008. Seasonal and interannual variation of streamflow pathways and biogeochemical implications in semi-arid, forested catchments in Valles Caldera, New Mexico. Ecohydrology 1, 239–252.
Mahaut, V., De Bondt, K., Deligne, C., 2011. Interdisciplinary methodological approach for urabn water management in densely urbanized areas within Brussels. In: Bodart, M., Evrard, A. (Eds.), Architecture & Sustainable Development, Conference Proceedings of the 27th International Conference on Passive and Low Energy Architecture. Louvain-La-Neuve, July 2011. pp. 263–268.
Martin-Gomez, P., Barbeta, A., Voltas, J., Penuelas, J., Dennis, K., Palacio, S., Dawson, T.E., Ferrio, J.P., 2015. Isotope-ratio infrared spectroscopy: a reliable tool for the investigation of plant-water sources? New Phytol. 207, 914–927.
Panasiuk, O., Hedström, A., Marsalek, J., Ashley, R.M., Viklander, M., 2015. Contamination of stormwater by wastewater: a review of detection methods. J. Environ. Manage. 152, 241–250.
Penckwitt, J., van Geldern, R., Hagspiel, B., Packebusch, B., Mahr, A., Burkhardt, K., Barth, J.A.C., 2016. Quantification of groundwater infiltration into urban sewer systems using stable isotopes. Grundwasser 21, 217–225.
Prüss, A., 1998. Review of epidemiological studies on health effects from exposure to recreational water. Int. J. Epidemiol. 27, 1–9.
Prigiobbe, V., Giulianelli, M., 2009. Quantification of sewer system infiltration using $\delta^{18}O$ hydrograph separation. Water Sci. Technol. 60 (3), 727–735.
Rozanski, K., 1985. Deuterium and oxygen-18 in European groundwaters –links to atmospheric circulation in the past. Chem. Geol. 52, 349–363.
Schilperoort, R., Meijer, H., Flamink, C., Clemens, F., 2007. Changes in isotope ratios during domestic wastewater production. Water Sci. Technol. 55 (4), 93–101.
Schilperoort, R., 2004. Natural Water Isotopes for the Quantification of Infiltration and Inflow in Sewer Systems, Msc Thesis. Delft university of Technology (151 p).
Schulte, P., van Geldern, R., Freitag, H., Karim, A., Négrel, P., Petelet-Giraud, E., Probst, A., Probst, J.-L., Telmer, K., Veizer, J., Barth, J., 2011. Applications of stable water and carbon isotopes in watershed research: weathering, carbon cycling, and water balances. Earth Sci. Rev. 109, 20–31.
Schwarzenbach, R.P., Egli, T., Hofstetter, T.B., von Gunten, U., Wehrli, B., 2010. Global water pollution and human health. Annu. Rev. Environ. Resour. 35, 109–136.
Singleton, G., Coplen, T., Qi, H., Lorenz, J., 2009. Laser-based stable hydrogen and oxygen analyses: How reliable can measurement results be? Geophysical Research Abstracts, EGU General Assembly 2009 11, 3290.
Staufer, P., Scheidegger, A., Rieckermann, J., 2012. Assessing the performance of sewer rehabilitation on the reduction of infiltration and inflow. Water Res. 46, 5185–5196.
Vazquez-Sune, E., Carrera, J., Tubau, I., Sanchez-Vila, X., Soler, A., 2010. An approach to identify urban groundwater recharge. Hydrol. Earth Syst. Sci. 14, 2085–2097.
Vivaqua, 2012. In: Leaflet, Franck Ch. (Ed.), Tailfer: the Technology Serving the Water (in French), (3p., http://www.vivaqua.be/sites/default/files/tailfer_la_technologie_au_service_de_leau.pdf, Accessed January 2018).
Walsh, C., Fletcher, T., Burns, M., 2012. Urban stormwater runoff: a new class of environmental flow problem. PLoS One 7 (9), 1–10.
Weiss, G., Brombach, H., Haller, B., 2002. Infiltration and inflow in combined sewer systems: long-term analysis. Water Sci. Technol. 45, 11–19.
West, A., Goldsmith, G., Brooks, P., Dawson, T., 2010. Discrepancies between isotope ratio infrared spectroscopy and isotope ratio mass spectrometry for the stable isotope analysis of plant and soil waters. Rapid Commun. Mass Spectrom. 24, 1948–1954.
de Ville, N., Le, H.M., Schmidt, L., Verbanck, M.A., 2017. Data-mining analysis of in-sewer infiltration patterns: seasonal characteristics of clear water seepage into Brussels main sewers. Urban Water J. 14 (10), 1090–1096.
van Geldern, R., Barth, J.A.C., 2012. Optimization of instrument setup and post-run corrections for oxygen and hydrogen stable isotope measurements of water by isotope ratio infrared spectroscopy (IRIS). Limnol. Oceanogr. Methods 10, 1024–1036. https://doi.org/10.4319/lom.2012.10.1024.